ÇUKUROVA UNIVERSITY
INSTITUTE OF NATURAL AND APPLIED SCIENCES

MSc. THESIS

Mert LÜYE

DESIGN BASED ON DYNAMIC ANALYSIS OF BOOM-STICK GROUP IN BACKHOE LOADERS

DEPARTMENT OF MECHANICAL ENGINEERING

ADANA-2022

ABSTRACT

MSc. THESIS

DESIGN BASED ON DYNAMIC ANALYSIS OF BOOM-STICK GROUP IN BACKHOE LOADERS

Mert LÜYE
ÇUKUROVA UNIVERSITY
INSTITUTE OF NATURAL AND APPLIED SCIENCES DEPARTMENT OF MECHANICAL ENGINEERING

Supervisor	:	Asst. Prof. Dr. Mehmet İlteriş SARIGEÇİLİ
		Year: 2022, Pages: 92
Jury	:	Asst. Prof. Dr. Mehmet İlteriş SARIGEÇİLİ
	:	Assoc. Prof. Dr. Erinç ULUDAMAR
	:	Asst. Prof. Dr. Durmuş Ali BİRCAN

Backhoe loader or backhoe loader machinery is a work machine equipped with a bucket on the tractor body in front and a small backhoe on the back. It is used in works such as loading, transporting and digging various materials. Since backhoe loader machines have versatile working capability, the positions of the parts that make up the design and the force values that occur in each position can differ. With the help of the free body diagram, the reaction forces at joints can be calculated with respect to time for any boom and stick position. However, it takes a long time to do this for positions corresponding to each time, and the presence of these variables makes it difficult to examine the boom and stick design group in terms of stress. In this study, which was carried out with the finite element method, the critical position determination of the backhoe design of a backhoe loader machine was made with the help of dynamic analysis at full capacity load. By taking the determined critical position as a reference, the parts to be reduced in weight were determined by static analysis. A total of 32 kg lighter backhoe group was designed and static, modal, vibration and shock analyses were applied to this new design, respectively. The lightweight backhoe design with the boundary conditions created with reference to military standards of MIL-STD-810G was structurally examined in detail and it was determined that it was durable under operating conditions.

Keywords: Backhoe, boom, stick, FEA, dynamic, structural, modal, vibration, shock, MIL-STD-810G

ÖZ

YÜKSEK LİSANS TEZİ

KAZICI YÜKLEYİCİLERDE BOM-STIK GRUBUNUN DİNAMİK ANALİZE DAYALI TASARIMI

Mert LÜYE

ÇUKUROVA ÜNİVERSİTESİ
FEN BİLİMLERİ ENSTİTÜSÜ
MAKİNE MÜHENDİSLİĞİ ANABİLİM DALI

Supervisor	:	Dr. Öğretim Üyesi Mehmet İlteriş SARIGEÇİLİ
		Yıl: 2022, Sayfa: 92
Jury	:	Dr. Öğretim Üyesi Mehmet İlteriş SARIGEÇİLİ
	:	Doç. Dr. Erinç ULUDAMAR
	:	Dr. Öğretim Üyesi Durmuş Ali BİRCAN

Backhoe loader ya da kazıcı yükleyici makineler, traktör gövdesi üzerinde önünde kova ve arka tarafında küçük bir kazıcı ile donatılmış bir iş makinasıdır. Çeşitli malzemeleri yükleme, taşıma, kazma gibi işlerde kullanılmaktadır. Backhoe loader makineler çok yönlü çalışma kabiliyetine sahip olduklarından tasarımı oluşturan parçaların aldıkları konumlar ve her konumda oluşan kuvvet değerleri farklılık gösterebilmektedir. Serbest cisim diyagramı yardımıyla her bir zamana denk gelen boom ve stick pozisyonu için mafsallardaki tepki kuvvetleri hesaplanabilir. Ancak bu işlemi her bir zamana denk gelen pozisyonlar için yapmak uzun süreler almakta ve bu değişkenlerin varlığı bom ve stick tasarım grubunu gerilme açısından incelemeyi zorlaştırmaktadır. Sonlu elemanlar yöntemiyle yapılan bu çalışmada bir backhoe loader makineye ait backhoe tasarımının tam kapasite yüklü durumda dinamik analiz yardımıyla kritik konum tespiti yapılmıştır. Tespit edilen kritik konum referans alınarak statik analiz ile hafifletme yapılacak parçalar tespit edilmiştir. Toplamda 32 kg daha hafif bir backhoe grubu tasarlanmıştır ve bu yeni tasarıma sırasıyla statik, modal, titreşim ve şok analizleri uygulanmıştır. Askeri standartlar referans alınarak oluşturulan sınır şartları ile hafifletilmiş backhoe tasarımı yapısal olarak ayrıntılı bir şekilde incelenmiştir ve çalışma şartları altında mukavim olduğu tespit edilmiştir.

Anahtar kelimeler: Kazıcı yükleyici, bom, kol, sonlu elemanlar yöntemi, dinamik, yapısal, doğal frekans, titreşim, MIL-STD-810G

EXPANDED ABSTRACT

Backhoe loader or backhoe loader machinery is a work machine equipped with a bucket on the tractor body in front and a small backhoe on the back. It is used in works such as loading, transporting and digging various materials. Since backhoe loader machines have versatile working capability, the positions of the parts that make up the design and the force values that occur in each position can differ. With the help of the free body diagram, the reaction forces at joints can be calculated with respect to time for any boom and stick position. However, it takes a long time to do this for positions corresponding to each time, and the presence of these variables makes it difficult to examine the boom and stick design group in terms of stress.

In this study, critical position determination was made with the help of dynamic analysis of the backhoe design of a backhoe loader machine in full load condition which was carried out with the finite element method by using the Transient Analysis module in the Ansys Workbench program. The position analysis of the determined critical position was expressed with formulas and the model to be used in the analyses was established. The current backhoe design has been statically analyzed at the same boundary conditions and focused on the boom design group to which weight reduction is planned. Static analysis results were examined and it was determined that the equivalent stresses occurred were below the yield strength of the relevant material (S355J2). As a result of the determinations made, it is aimed to obtain a 32 kg lighter backhoe design by reducing the existing thicknesses of the boom wall sheet and boom lower cross member sheets in the boom design group by 4 mm.

The lightweight backhoe design was remodeled at the critical position determined to structurally examine and validate the design under operating conditions. Applying vibration and shock analyses to the new design with reference to static, modal and military standards (MIL-STD-810G), respectively, a model was established for each analysis. While establishing the models, attention was paid to

ensure that the boundary conditions used in the current design were the same in order to make a healthy comparison.

When the static analysis results of the lightweight design were examined, it was observed that the highest equivalent stress value occurred as 46.601 MPa. It has been determined that the relevant material that maked up the boom design group had a value far below it. Modal analysis was performed in preparation for vibration and shock analysis. The natural frequencies of the backhoe design, which was analyzed with 30 modes, were determined. As a result of the modal analysis, the mass participation rates of the design were determined to be above 90% for the X, Y and Z axes separately. With its high mass participation rates, it supported the accuracy of vibration and shock analysis results in accordance with military standards.

The results of the vibration analyses carried out in each axis direction were examined and equivalent stresses were observed below the yield strength of the relevant material. Vibration loads applied to the design were applied for 3600 s and damage formation was investigated. It has been determined that the damage values for each axis, X, Y and Z, are below 1.

The maximum equivalent stresses resulting from the shock analysis were determined and the behavior of the lightweight backhoe design under sawtooth shock loads was investigated. It was read as 721.39 MPa, 592.99 MPa and 677.19 MPa on each axis, X, Y and Z, respectively. It has been foreseen that the detected equivalent stresses would not pose a structural problem due to the fact that they are not spread over the whole design. It has been observed by examining the time dependent stress graphs that the design, which was subjected to shock loads, absorb the loads.

The lightweight backhoe design was examined with static, modal, vibration and shock analyses and it was determined that 32 kg of lightening would not pose a problem in terms of strength. Due to the investigations carried out in this thesis, a 32 kg lighter backhoe design has been obtained.

GENİŞLETİLMİŞ ÖZET

Backhoe loader ya da kazıcı yükleyici makineler, traktör gövdesi üzerinde önünde kova ve arka tarafında küçük bir kazıcı ile donatılmış bir iş makinasıdır. Çeşitli malzemeleri yükleme, taşıma, kazma gibi işlerde kullanılmaktadır. Backhoe loader makineler çok yönlü çalışma kabiliyetine sahip olduklarından tasarımı oluşturan parçaların aldıkları konumlar ve her konumda oluşan kuvvet değerleri farklılık gösterebilmektedir. Serbest cisim diyagramı yardımıyla her bir zamana denk gelen boom ve stick pozisyonu için mafsallardaki tepki kuvvetleri hesaplanabilir. Ancak bu işlemi her bir zamana denk gelen pozisyonlar için yapmak uzun süreler almakta ve bu değişkenlerin varlığı boom ve stick tasarım grubunu mukavemet açısından incelemekte güçlük çıkarmaktadır.

Bu çalışmada, bir backhoe loader makineye ait backhoe tasarımının tam kapasite yüklü durumda dinamik analiz yardımıyla kritik konum tespiti Ansys Workbench programında Transient Analysis modülü kullanılanarak sonlu elemanlar yöntemiyle yapılmıştır. Tespit edilen kritik konum referans alınarak statik ve diğer analizlerde kullanılacak model kurulmuştur. Mevcut backhoe tasarımı statik olarak aynı sınır şartlarında analiz edilmiştir ve hafifletme yapılması planlanan bom tasarım grubuna odaklanılmıştır. Statik analiz sonuçları incelenmiştir. Meydana gelen eşdeğer gerilmelerin ilgili malzemenin (S355J2) akma dayanımının altında kaldığı tespit edilmiştir. Yapılan tespitler sonucu bom tasarım grubunda bulunan bom duvar sacı ve boom alt travers saclarının mevcut kalınlıklarından 4 mm azaltılarak 32 kg daha hafif bir backhoe tasarımı elde edilmesi hedeflenmiştir.

Hafifletilmiş backhoe tasarımı, çalışma şartları altında tasarımı yapısal olarak incelemek ve doğrulamak için tespit edilen kritik konumda tekrar modellenmiştir. Yeni tasarıma sırasıyla statik, modal ve askeri standartlar (MIL-STD-810G) referans alınarak belirlenen titreşim ve şok analizleri uygulanarak her analiz için bir model oluşturulmuştur. Modeller oluşturulurken, sağlıklı bir karşılaştırma yapılabilmesi için mevcut tasarımda kullanılan sınır şartlarının aynı olmasına dikkat edilmiştir.

Hafifletilmiş tasarıma ait statik analiz sonuçları incelendiğinde meydana gelen en yüksek eşdeğer gerilme değerinin 46.601 MPa olarak meydana geldiği gözlenmiştir. Bom tasarım grubunu oluşturan ilgili malzemenin çok altında bir değer olduğu tespit edilmiştir. Tireşim ve şok analizlerine hazırlık olarak modal analiz yapılmıştır. 30 mode ile analizi gerçekleştirilen backhoe tasarımının doğal frekansları tespit edilmiştir. Modal analiz sonucu tasarımın kütle katılım oranları X, Y ve Z eksenleri için ayrı ayrı %90 üzerinde olarak tespit edilmiştir. Yüksek kütle katılım oranları ile, askeri standartlara uygun titreşim ve şok analiz sonuçlarının doğruluğunu desteklemiştir.

Her bir eksen doğrultusunda gerçekleştirilen titreşim analizleri sonuçları incelenmiş ve ilgili malzemenin akma dayanımının altında eşdeğer gerilmeler gözlemlenmiştir. Tasarıma uygulanan titreşim yükleri 3600 s boyunca uygulanarak hasar oluşumu incelenmiştir. X, Y ve Z eksenlerinin her biri için hasar değerlerinin 1’ in altında olduğu tespit edilmiştir.

Şok analizinden kaynaklanan maksimum eşdeğer gerilmeler belirlenmiş ve hafif beko tasarımının testere dişi şok yükleri altındaki davranışı araştırılmıştır. X, Y ve Z eksenlerinde sırasıyla 721.39 MPa, 592.99 MPa ve 677.19 MPa olarak okunmuştur. Tespit edilen eşdeğer gerilmelerin tasarımın bütününe yayılı olmaması nedeniyle yapısal bir sorun teşkil etmeyeceği öngörülmüştür. Şok yüklere maruz kalan tasarımın yükleri sönümlediği zamana bağlı gerilme grafikleri incelenerek gözlemlenmiştir.

Hafifletilmiş backhoe tasarımı statik, modal, titreşim ve şok analizleri ile incelenerek gerçekleştirilen 32 kg hafifletmenin mukavemet açısından bir sorun teşkil etmeyeceği tespit edilmiştir. Bu tez çalışmasında gerçekletirilen incelemeler sayesinde 32 kg daha hafif bir backhoe tasarımı elde edilmiştir.

ACKNOWLEDGEMENTS

I would like to thank my supervisor Asst. Prof. Dr. Mehmet İlteriş SARIGEÇİLİ. I am grateful and indebted to him for his assistance, valuable guidance, and encouragement extended to me.

I must express my very profound gratitude to my parents who have always been with me and given their unending support.

TABLE OF CONTENTS **PAGE**

LIST OF TABLES **PAGE**

LIST OF FIGURES **PAGE**

LIST OF ABREVIATIONS

FEM	: Finite element method
FEA	: Finite element analysis
CAD	: Computer aided design
DOF	: Degree of freedom
P	: Pressure
CAE	: Computer aided engineering
BCs	: Boundary conditions
SPCs	: Single point constraints
MPCs	: Multi point constraints
ICA	: Initial condition analysis
KA	: Kinematic analysis
RBE	: Rigid body element
MBD	: Multi body dynamic
g	: Gravitational Acceleration
F	: Force in bucket
PSD g	: Power spectral densities
Steinberg	: Method selection theory
KA	: Kinematic analysis
RBE	: Rigid body element
MBD	: Multi body dynamic
S1	: Boom cylinder distance
S2	: Stick cylinder distance
S3	: Bucket cylinder distance

XIX

1. INTRODUCTION

Backhoe loader is a construction machine equipped on a tractor body with a bucket at the front and a small backhoe at the rear (Figure 1.1). It is used in works such as loading, transporting and digging various materials. The movement of the backhoe loader, loading and excavator part is carried out by the hydraulic system. It is one of the most used tools in construction machinery. The loader front bucket part is used to pick up any material from one place and load it to another place in a short distance. It is not suitable for long-distance freight transportation. The excavator part is used for trench excavations, channel excavations, building foundations and loading operations.

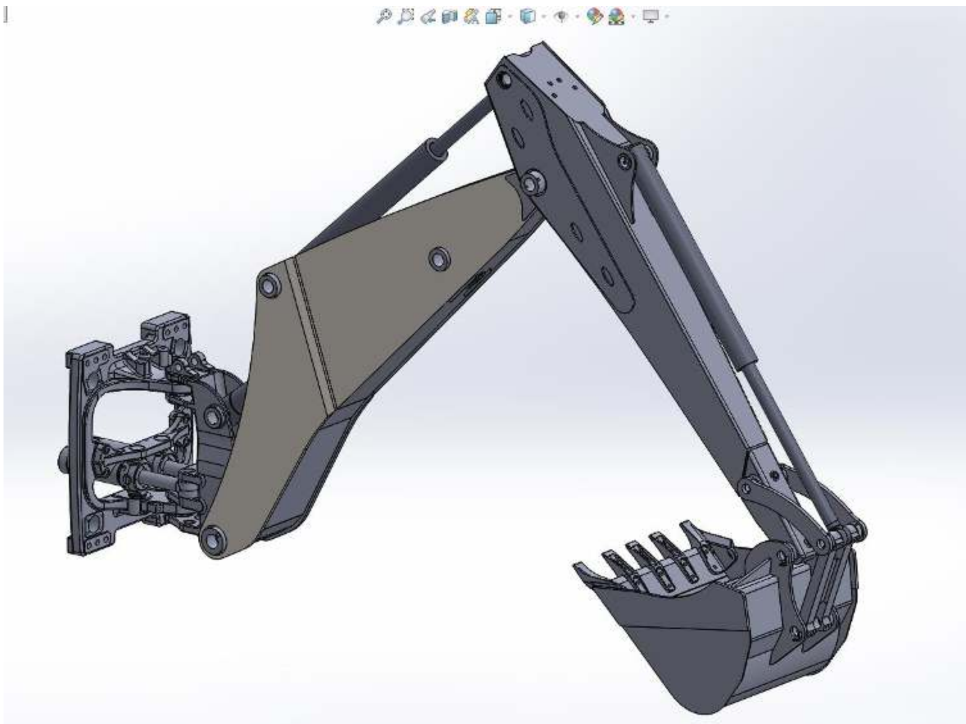

Figure 1.1. Boom stick design of backhoe loader

Since backhoe loader machines have versatile working capability, the positions of the components that constitute the design and the interaction force values that occur in each position can differ. For this reason, it would be more accurate to determine the positions of the arms (boom and stick) according to angular values and examine them at these positions. With the help of free body diagram, the reaction forces at joints can be calculated for each boom and stick position dependent on time. However, it takes a long time to perform these calculations for every position taken throughout the operation time interval, and the presence of these variables makes it difficult to examine the boom-stick design group for strength. On the other side, design groups can be examined in terms of strength as close to reality as possible with dynamic analysis where variable parameters are defined depending on time. Studies on the structural analysis of backhoe loaders are increasing in the literature. Previous studies mostly focused on static and kinematic analysis. The difference of this study from previous studies is to determine the critical position of the backhoe group under load during operation with the help of dynamic analysis in addition to static and kinematic analysis. A light weight design is obtained by performing static, natural frequency, random vibration and dynamic-based shock analysis suitable for military conditions on the model established with reference to the critical position. Inputs used in vibration and shock analysis for a backhoe design conforming to military standards have been determined with reference to MIL-STD-810 (MIL-STD-810).

The MIL-STD-810 test method standard for environmental engineering topics and laboratory testing is a publication of the US Department of Defense with contributions from the US Army, Air Force, and Navy, as well as the Institute of Environmental Science and Technology (IEST). The Shock and Vibration Information Analysis Center (SAVIAC) adapts the environmental design and test limits of a material to the conditions that a particular material will experience throughout its service life, and states that laboratory test methods should be established that replicate the effects of the environments on the material, rather than trying to replicate the environments themselves.

The MIL-STD-810 standard is designed to rely on the environmental value and durability of material system designs and provides test methods to achieve the following purposes:

- defining environmental stress sequences, durations and equipment lifecycle levels,
- developing analysis and test criteria suitable for the material and environmental life cycle,
- evaluating material performance when exposed to life cycle environmental stresses,
- identifiying deficiencies in material design, materials, manufacturing processes, packaging techniques, and maintenance methods.

The vibration test protocol reproduces the types of forces that will occur over the working life of a product. Random vibration testing can detect weaknesses in the design and can be used in jet engines, cruise missiles, catalytic converters, motorcycle components, and any product or construction equipment designed for transportation. MIL-STD-810 covers a set of vibration tests that provide different procedures depending on whether vibration is expected during manufacture, shipping, or operation. Tests should be performed in environments set up in accordance with best practices for isolation mass, inertial mass, and reaction mass. In addition, tests must be carefully calibrated to compensate for the influence of ambient vibrations on the test process. Random vibration loads are defined in Figure 514.7C-2 of the Method 514.7C-I, (Common carrier, US highway truck vibration exposure). With respect to this method in the standard, vibration loads are applied for 3600 seconds.

Shock testing can determine whether devices can withstand the high-level shocks and temperature changes encountered during shipping and handling. During testing, a device is subjected to sudden and excessive acceleration or deceleration.

Engineers analyze device responses to determine performance quality. Shock and vibration testing for electrical components, black boxes, antennas, hydraulic components and material samples can be made. The following methods are used for mechanical shock testing: pyrotechnics to simulate pyroshock, drop testing, drop towers to induce mechanical shock, airgun generated hydroshock, free fall, and variable force testing techniques. Based on the military standard (MIL-STD-810G), only two classical shock pulses are defined for testing: the terminal peak sawtooth pulse and the trapezoidal pulse. The terminal peak sawtooth pulse along with its parameters and tolerances are provided on Figure 516.6-10. The sawtooth shock loads of 15.2g are applied as stated in Method 516.7.

The data used and determined in vibration and shock tests are used as input in vibration and shock analysis in the finite element method and make a great contribution to determining the boundary conditions of the analysis model. Thus, it is possible to have a prediction with structural analyses using MIL-STD-810 data before the physical tests are performed. MIL-STD-810 includes very comprehensive test procedures and data. In this thesis, mostly highway vibration profiles and sawtooth shock profiles that vehicles are exposed to as a result of sudden accelerations are used.

2. PREVIOUS STUDIES

In the literature, there are many studies on the design and analysis of backhoe loader. Most of these studies concentrate on the design and improvement based on static analysis related to the boom-stick group using finite element method (FEM). In addition, time-dependent dynamic analysis, vibration and shock analysis are not included.

The analysis of the boom and arm group of a backhoe loader machine and the improvement of the stresses due to the forces were presented by (Özsaraç, E., 2016). In that study, in addition to keeping the forces acting on the product below the desired limit values depending on the forces it was exposed to, the product was required to meet these loads with optimum raw material use. Firstly, the force analysis was completed. The front attachment was then modeled and analyzed according to the critical position of the machine. Improvements were applied according to the results. FEM is used as a numerical solution method for this engineering problem. Finite element analysis (FEA) were made with Simxpert package program.

Oyman (2005) stated in his study that since the hardware was in direct interaction with the workpiece, it was exposed to reaction forces during operation, and therefore the force analysis of the parts had an important place during the design. Therefore, the force analysis of the system began by first defining the reaction force acting on the bucket. Then the free body diagram of each part was drawn and the stress states were revealed. Finally, strength checks were made according to the stress state of each part, and the final shape of the parts were given.

Yeter (2009) conducted a study in which the back and forearms of a backhoe-loader were analyzed and improvements were aimed according to the analysis results. Firstly, FEA was performed according to the reaction forces of the arm hinges calculated according to the maximum piston forces, and then the maximum loads calculated according to the symmetrical and unsymmetrical boundary conditions. In order to reduce the stress in the regions of stress intensity, reinforcements were made and FEA was performed again. In the FEA, Ansys Workbench finite element package program was used.

Since backhoe manufacturers offer boom-stick groups with different digging distances to their customers as an option in their models, (Özer, S., 2007) conducted stress analyses on boom-stick groups with different digging distances using the FEA method. A correlation was established between the shape parameters of the stick groups. With the help of this relationship, boom-stick groups with different digging distances could be designed automatically in Solidworks program. FEA was carried out in the Ansys Workbench program.

The complexity and constraints imposed on the loading mechanism do not allow the use of classical optimization techniques used in the synthesis of mechanisms. While meeting the constraints as well as trying to maximize the shear forces that the machine can produce, (İpek, L., 2006) presented a study that used genetic algorithms to determine the values of the design parameters of the mechanism. Therefore, a computer program was aimed to develop for optimizing the performance of the computer.

Yener (2005) presented a computer interface that connected the user to the commercial FEA program "MSC.Marc-Mentat" to perform automatic FEA of an excavator boom using the DELPHI platform. To add some flexibility to the interface called OPTIBOOM, the boom geometry was parameterized. Parametric FEA of a boom shortens the design steps and helps find the optimum design in terms of stresses and mass.

Özünlü (2009) showed dynamic force analysis while digging the ground of an excavator with 3 degrees of freedom and the motion was simulated on the computer screen. Since the standard load calculations were made statically, the effects of time-varying forces on the system could not be observed. The dynamic analysis method used in this study was the Recursive Newton – Euler Method and the numerical analysis method for simulation was the 4th Order Runge – Kutta

Method. By this study, the effects of sudden speed changes, i.e. accelerated movements, positions of bodies and dynamic forces at points would be assigned in construction machines and it would be possible to plan and control the movement.

Kocabıyık (2010) presented the previously designed protective cabin to be tested according to ISO standards. CATIA V5 three-dimensional design software was used during modelling. Ansys software was used to create the finite element model, and the AUTODYN engineering software was used to perform the calculations and display the results. Thus, the safety requirements of the construction equipment cabin were tested.

Kılınç (2009) developed a dynamic model of the loader system of a backhoe-loader. Rigid bodies and connections in the loader mechanism and loader hydraulic system components were modeled and analyzed in the same environment using physical modeling toolboxes in the commercially available simulation software MATLAB/Simulink. The interaction between the bodies and the response of the hydraulic system were achieved by the combined work of mechanical and hydraulic analysis. System variables such as pressure, flow, and displacement were measured on a physical machine and then compared with simulation results. The simulation results were in agreement with the measurement results. The main result of this work was the ability to determine the dynamic loads on the backhoe loader's joints and attachments. In addition, prototyping time and costs could be greatly reduced by implementing this model in the design process.

In another study, Sharma (2005) carried out kinematic analysis of the boom and stick of the excavator and then performed stress analysis using the FEM. He made improvements in the design of boom and stick based on the results of FEA. Stick and boom analyses were performed separately. Commercial Mathcad and Design View programs were used in computer environment to find the forces acting on the boom and stick due to separate analyses. The forces found in the FEA were applied to the hydraulic piston bearings of the boom and stick. Solid models were prepared in Solid Edge program, finite element mesh was created in Hypermesh program and analyses were performed by applying boundary conditions and forces in Ideas program. As a result of the improvements made, the stresses in the stick were reduced to around 220 MPa, which is the reliable limit, and the mass of the stick was reduced from 409 kg to 387.4 kg. With the improvements made in the boom, the stresses were reduced to around 220 MPa, which was the reliable limit, but the weight of the boom increased from 678 kg to 712 kg.

By Dağ et al. (2005), a parametric three-dimensional FEM of an excavator boom with a capacity of 22 tons (i.e. HMK220LC-2 model, manufactured by Hidromek Company) was developed, and fatigue calculations were made by considering the critical stresses in different designs obtained from the analysis. The fatigue life differences between the obtained results and the design geometries were investigated.

In this study, a different perspective was brought to the analyzes made by the FEM method with the Taguchi method. CAD programs were used for the 3D data used in the FEM model. In this study, the maximum bucket breakout force of the excavator was calculated as 123.4 kN. The calculated force was used to determine the boundary conditions in the FEM model. By making geometric and thickness changes, 639 FEA results were obtained and the design with the least stress was determined among these results.

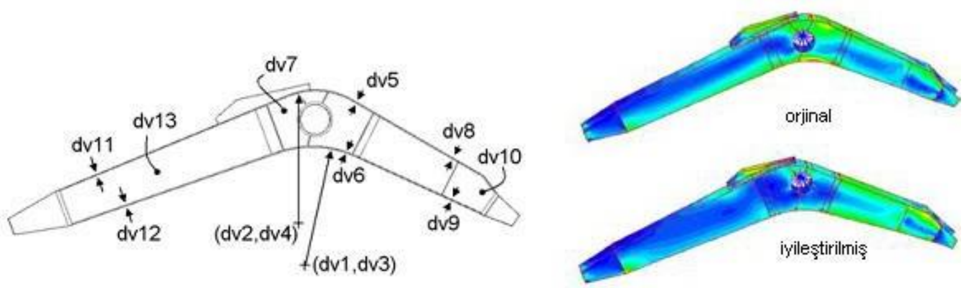

Figure 2.1. Parameters and Equivalent Stress (Frimpong, S., 2007)

Stresses and deformations during operation in the boom of a cable bucket were investigated dynamically by Frimpong and Li (2007) using Adams-Nastran and Adams-Flex programs. By finding the stress distributions in the boom with FEM, critical regions were determined and basic data were obtained for future failure and fatigue analysis.

In order to verify the strength calculations obtained from FEM in construction machinery construction, experimental strength analyzes and comparisons were made by (Fıçıcı, F., 2003). In the preliminary stage of the experiment, the forces to be applied were determined with the help of kinematic analyzes of the mechanisms of the excavator load machines. Experimental location and boundary conditions have been determined. The determined boundary conditions were transferred to the analysis model made in the computer environment. As a result of FEA, the detection of critical regions and high stresses were determined. The stress values read as a result of FEM were read with strain gauges to compare the stress values read as a result of the experiments. As a result, it was seen that the FEM results made in the computer environment and the experimental stress results overlapped.

Since it is very difficult to carry out large-scale structural analysis and designs with a single computer, commercial programs now allow the analysis to be shared on more than one computer, with the advancing technology. An optimization approach for large-scale design problems by distributing processes via the internet has been applied by Lim (2005). One of the structures examined in the study was an excavator boom. When the analysis was done on a single computer, it took 94 minutes, and when it was distributed on 3 computers, it took 32.3 minutes. The boom was parametrically modeled and the boundary conditions were created by applying the maximum bucket breakout force to the boom with static calculations. The optimum model obtained as a result of the improvements made was 2.47% smaller in volume than the first model and the maximum stress was reduced from 256 MPa to 210 MPa.

Thorat et al. (2013) presented natural frequency identification of a backhoe loader chasis by carrying out modal analysis in Ansys Workbench. They also performed harmonic analysis in Ansys Workbench for obtaining vibration response at various locations of the chassis.

Vaniya et al. (2015) reviewed studies on FEA of backhoe chassis for reducing cost and weight. Xiaohuo et al. (Xiaohuo L., 2012) created complete 3D model of an excavator in Pro/E and performed the FEA in Ansys. The stress and deformation results were evaluated for the complete design.

Bhoomkar (2017) applied topology optimization for reducing weight of boom of a backhoe loader. Then, the stress and deformation levels were evaluated with static FEA to prove that the design was safe. As a result of the study, the weight of the boom was decreased by 5%.

Erklig and Yeter (2013) applied FEA for the improvement of the front loader arm and excavator boom designs under different loading conditions such as symmetrical and unsymetrical loading as well as cylinder active or inactive. In order to increase strength of the designs, various reinforcement parts were added and the results of FEA showed that strength of the arms was increased by nearly 20%.

Tewari et al. (2020) created 3D model of a physical excavator in PRO-E Wildfire V 5.0. Kinematic and dynamic analysis were performed in PRO-E Mechanica. FEA of the boom was carried out in Ansys for stress and deflection evaluation. Based on the obtained factor of safety results, the fatigue life of the boom was tried to be estimated.

When the previous studies are examined, it is noteworthy that there are many studies on the structural analysis of the backhoe loader machine with FEM. However, it is observed that the content of these studies is limited to static, kinematic and rigid body dynamics. As a main contribution of this study, the backhoe design will be evaluated based on static, kinematic and rigid body dynamics analysis, as well as vibration and shock analyses in accordance with military standards, which are also dynamically based.

3. MATERIAL AND METHOD

In this study, a computer with an AMD Ryzen 5 3600, 6-Core Processor, 3.60 GHz processor with a 64-bit Windows 10 operating system was used and the analyses were made using Static Structural, Modal, Transient Structural and Random Vibration modules in Ansys-Workbench R18.1 software. Solidworks and Autocad programs are utilized for technical drawing, measurement and 3D modeling.

Before examining the backhoe design with dynamic analysis, kinematic analysis was performed at the excavation starting position. The kinematic parameters such as the excavation starting position, velocity and acceleration in Figure 3.1 have been examined.

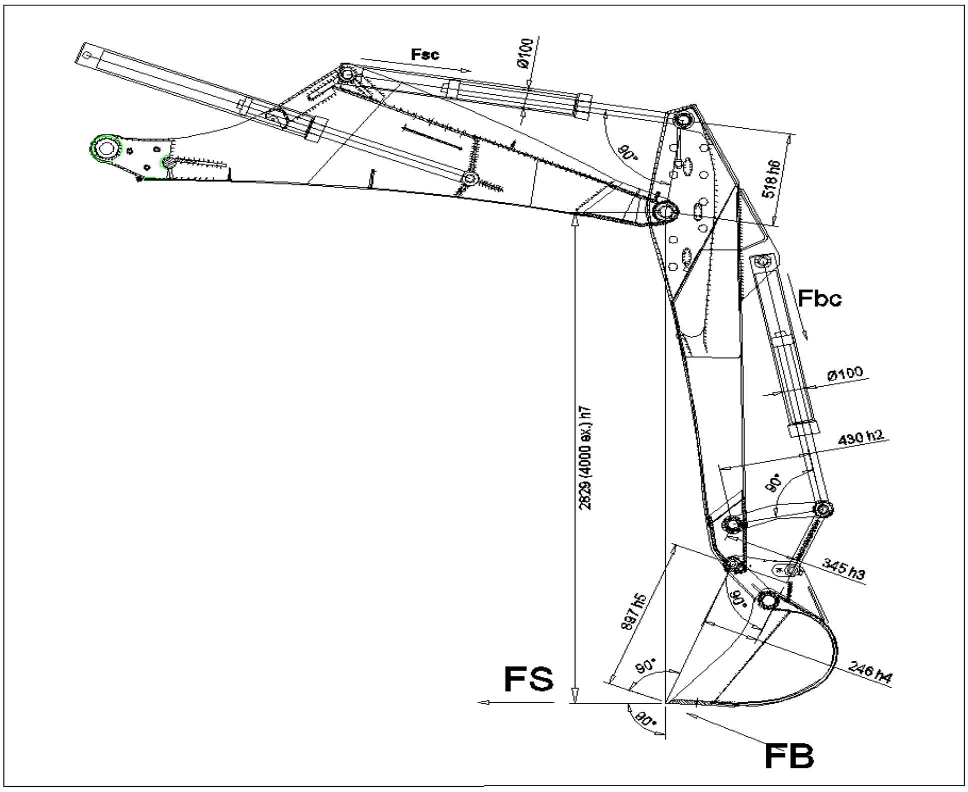

Figure 3.1. Bucket Tearout Force Position

The backhoe design has been dynamically analyzed to achieve critical position detection. It is aimed to support the dynamic analysis with the kinematic analysis of the starting position before the dynamic analysis. For position analysis, firstly, angles and lengths for boom, stick and bucket are defined. The visuals related to length and angle are given in Figure 3.2, Figure 3.3 and Figure 3.4. In Figure 3.2, AC shows the boom cylinder of length S_1 and BE the stick cylinder of length S_2. Points A and O are the pivot points where the boom attaches to the body. Your position of the boom relative to the X-axis is defined by the angle β_0. In order to calculate the β_0 angle, by applying the cosine theorem in the triangle OAC for the α_1 angle depending on the length $S_{1,}$ (as seen Eq. 3.1-3.3)

$$S_1^2 = l_0 + l_1^2 - 2 \times l_0 \times l_1 \times \cos \propto_1 \tag{3.1}$$

$$\propto_1 = \cos^{-1}\left(\frac{l_0^2 + l_1^2 + S_1^2}{2 \times l_0 \times l_1}\right) => \tag{3.2}$$

$$\beta_0 = \pi - \theta_0 - \alpha_1 => \tag{3.3}$$

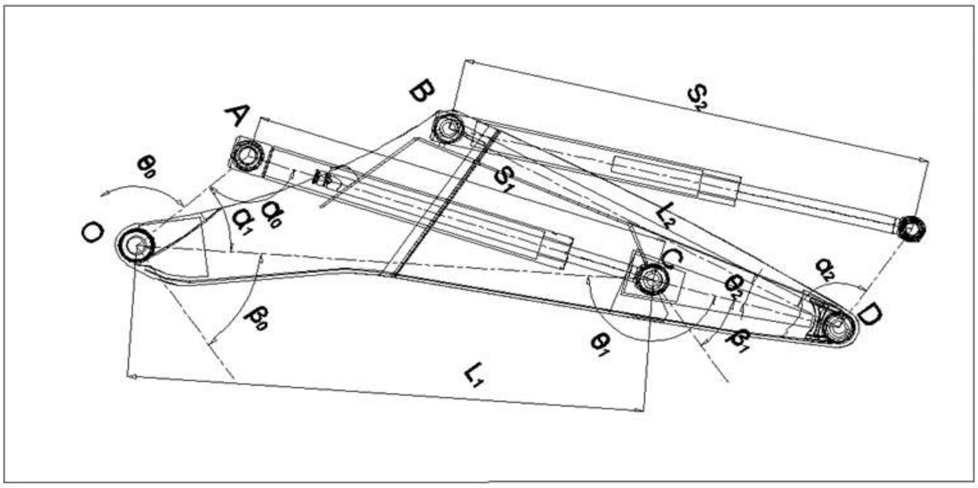

Figure 3.2. Position Analysis of Boom Design

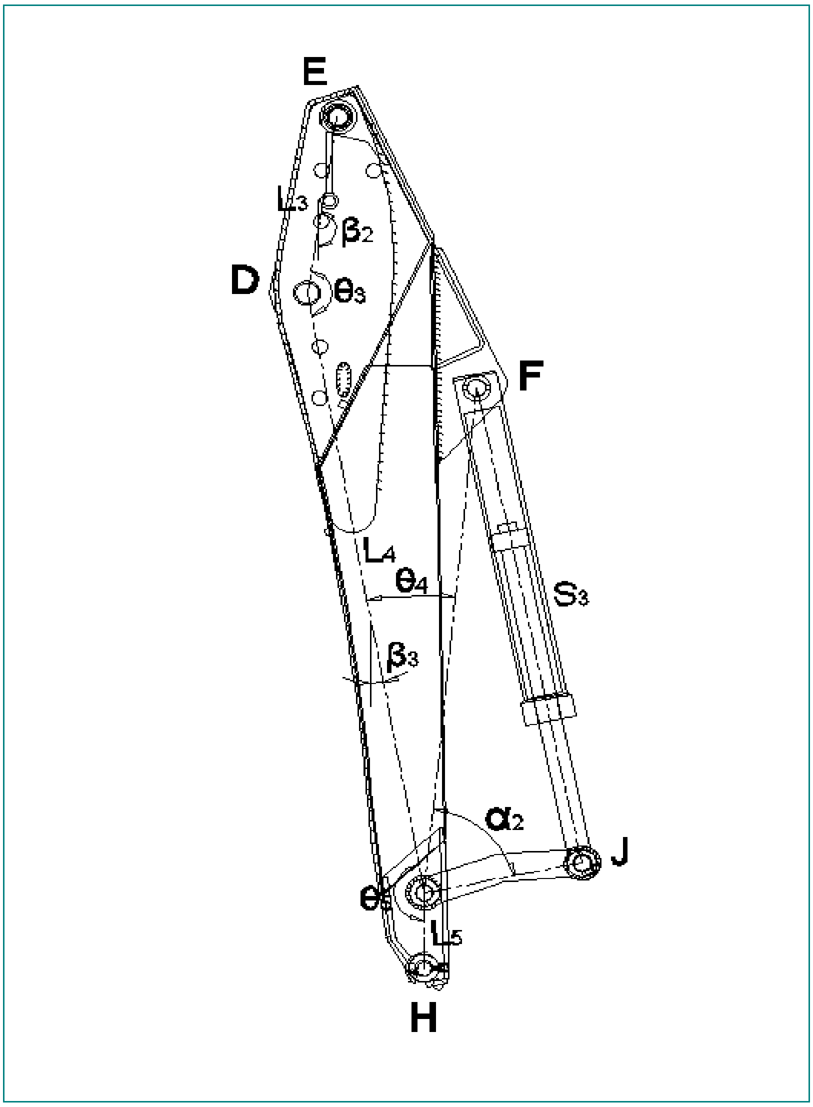

Figure 3.3. Position Analysis of Stick Design

In Figure 3.3 FJ shows the bucket cylinder of length S_3, D shows the boom stick attachment point, E shows the stick roller attachment point. The stick determines its position relative to the X-axis by the angle β2. If the following operations are performed to calculate this angle due to Eq. 3.4-3.6,

$$\propto_5 = \cos^{-1}\left(\frac{l_3^2 + l_2^2 + s_3^2}{2 \times l_3 \times l_2}\right) \tag{3.4}$$

$$\beta_1 = \theta_1 - \beta_0 \tag{3.5}$$

$$\beta_2 = \pi + \beta_1 - \theta_1 - \alpha_5 \tag{3.6}$$

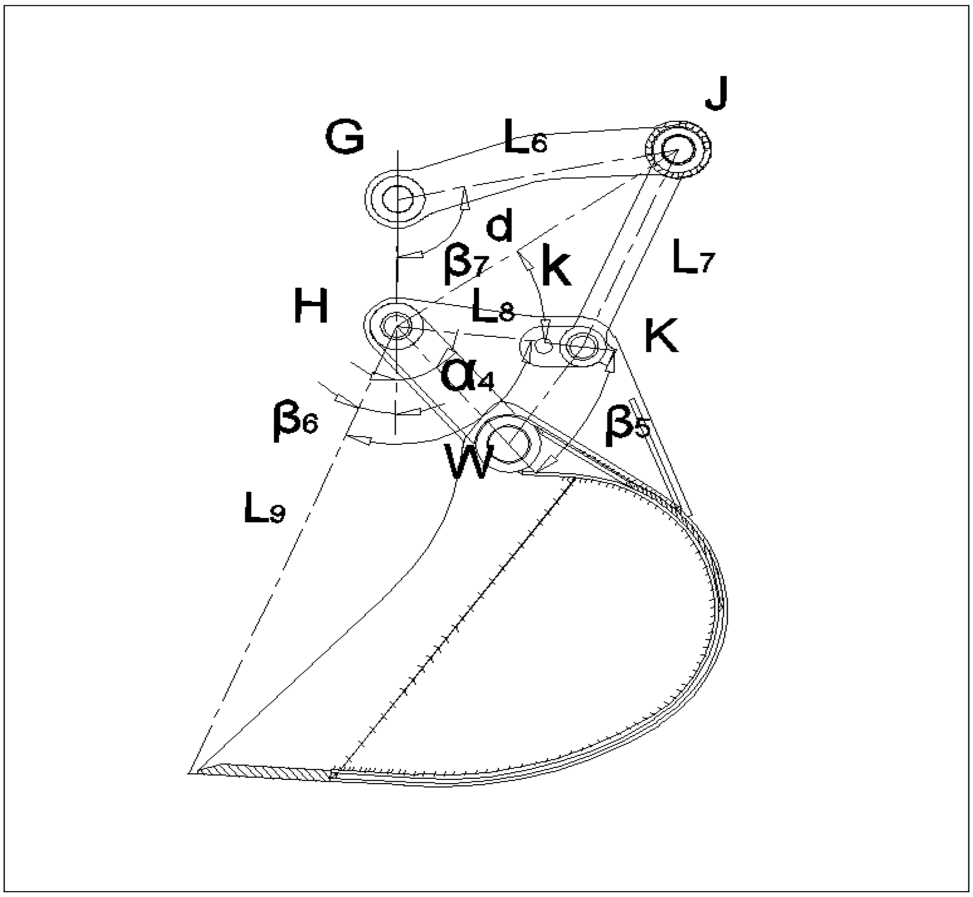

Figure 3.4. Position Analysis of Bucket Design

The bucket is the output member of the 4-rod GJKH mechanism. The bucket cylinder of length S_3 between FJ gives movement to the mechanism. In order to determine the position of the bucket, the position of the GJ crank must first be determined. Bucket and crank positions can be calculated with the help of the following equations 3.7-3.18:

$$S_3^2 = l_6^3 + l_4^2 - 2 \times l_6 \times l_4 \times \cos(\propto_2) \tag{3.7}$$

$$\propto_2 = \cos^{-1} \frac{l_6^2 + l_4^2 - s_3^2}{2 \times l_6 \times l_4} \tag{3.8}$$

$$\beta_3 = \beta_2 - \theta_3 \tag{3.9}$$

$$\beta_6 = \pi - \beta_3 - \alpha_2 - \theta_4 \tag{3.10}$$

$$xd = l_6 \times \cos \propto_3 - l_5 \tag{3.11}$$

$$yd = l_6 \times \sin \propto_3 \tag{3.12}$$

$$W = \propto \times \tan(\frac{yd}{xd})^2 \tag{3.13}$$

$$d = \sqrt{xd^2 + yd^2} \tag{3.14}$$

$$k = \cos^{-1}(\frac{l_8 + d^2 - l_7^2}{2 \times l_8 \times d}) \tag{3.15}$$

$$\propto_4 = W - k \tag{3.16}$$

$$\beta_4 = \beta - \pi + \theta_5 \tag{3.17}$$

$$\beta_5 = \beta_4 + \propto_4 \tag{3.18}$$

If link lengths and S_3 cylinder displacement are given, JG, JK and KH (bucket) positions can be calculated depending on the stick with the help of the above equations. Since the digging distance can be expressed as the sum of the projections of the lengths Km, OC, CD, DG, GH and HL on the X axis, Km is found with the help of the following equations 3.19 and 3.20.

$$\beta_6 = W - \propto_4 \tag{3.19}$$

$$Km = l_1 \times \cos\beta_0 + CD \times \cos\beta_1 + l_4 \times \cos\beta_3 + l_5 \cos\beta_5 + l_9 \times \cos\beta_9 \tag{3.20}$$

In addition to position analysis, velocity and acceleration i.e. kinematic analysis are performed. Schematic representation of the boom and hydraulic cylinder is shown in Figure 3.5. Based on the extension of the boom sylinder (s), the angular positions can be determined from Cosines Theorem as given in the following equations 3.21-3.24:

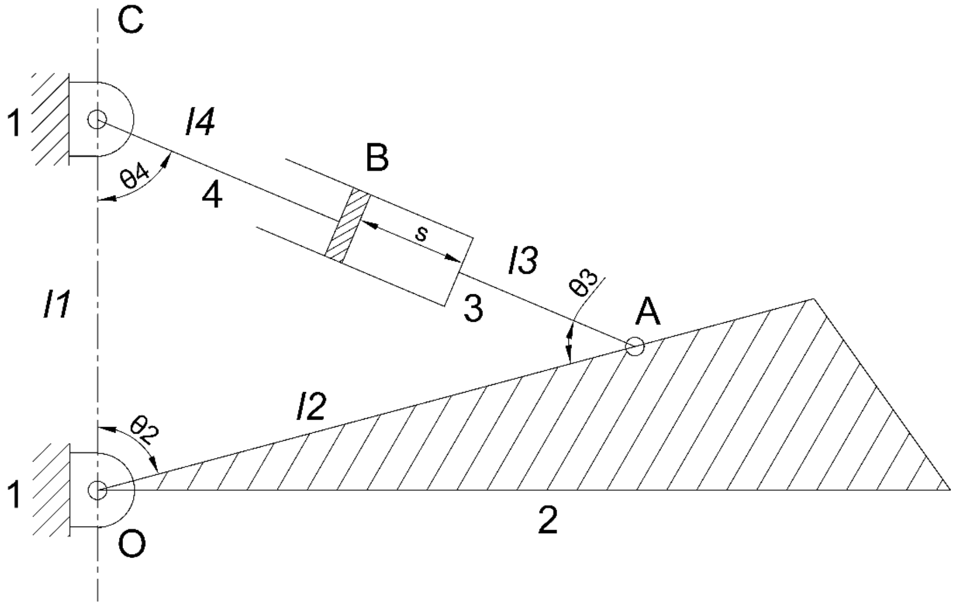

Figure 3.5. Schematic Representation of Boom Mechanism

$$l_1^2 = l_2^2 + (l_3 + l_4 + S)^2 - 2 \times l_2(l_3 + l_4 + S)\cos(\theta_3) \tag{3.21}$$

$$\theta_3 = \cos^{-1}(\frac{-l_1^2 + l_2^2 + (l_3 + l_4 + S)^2}{2 \times l_2 \times (l_3 + l_4 + S)}) \tag{3.22}$$

$$l_2^2 = l_1^2 + (l_3 + l_4 + S)^2 - 2l_1(l_3 + l_4 + S)\cos\theta_4 \tag{3.23}$$

$$\theta_4 = \cos^{-1}(\frac{-l_2^2 + l_1^2 + (l_3 + l_4 + S)^2}{2 \times l_1 \times (l_3 + l_4 + S)}) \tag{3.24}$$

The velocity polygon can be drawn as shown in Figure 3.6. Then, based on the cylinder piston velocity, the other unkown velocities can be calculated with help of equations 3.25-3.28:

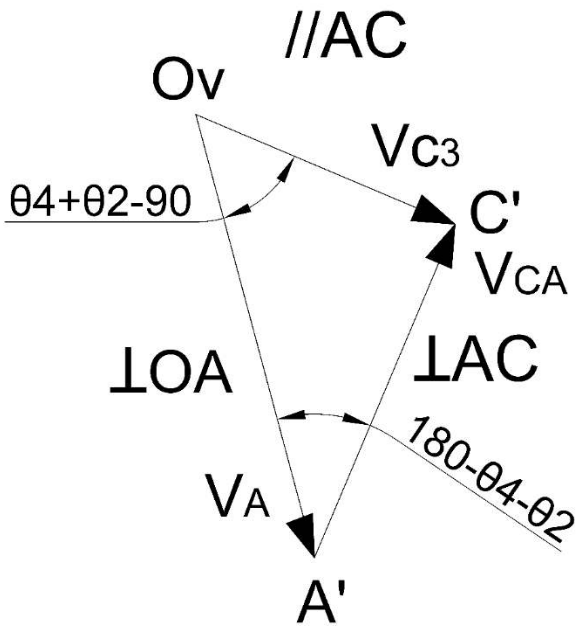

Figure 3.6. Boom Velocity Analysis

$$\overrightarrow{V_{c3}} = \overrightarrow{V_A} + \overrightarrow{V_{c3A}}\ ;\ V_{C3A} = V_{AC} \tag{3.25}$$

$$V_{AC} = \frac{V_{C3}}{\cos(\theta_4 + \theta_2 - 90)}\ ;\ V_{CA} = V_{C3} \times \tan(\theta_4 + \theta_2 + 90) \tag{3.26}$$

$$w_2 = \frac{V_A}{l_2};\ w_{CA} = \frac{V_{CA}}{(l_3 + l_4 + S)} = w_4 \tag{3.27}$$

$$\vec{V}_{C3} = Linear\ Piston\ Speed \tag{3.28}$$

The acceleration polygon can be drawn as shown in Figure 3.7. Then, depending on the cylinder-piston acceleration, other unknown accelerations can be calculated with the help of equations 3.29-3.39

$$\overrightarrow{a_{c3}} = \vec{a}_{c4n} + \vec{a}_{c4t} + \vec{a}_{c3c4n} + 2 \times \vec{V}_{c3c4} \times w_4 \tag{3.29}$$

$$\vec{a}_{c3} = \vec{a}_{An} + \vec{a}_{At} + \vec{a}_{c3An} + \vec{a}_{c3At} \tag{3.30}$$

$$\vec{a}_{c4n} + \vec{a}_{c4t} + \vec{a}_{c3c4n} + \vec{a}_{c3c4t} \times w_4 = \vec{a}_{An} + \vec{a}_{At} + \vec{a}_{c3An} + \vec{a}_{c3At} \tag{3.31}$$

$$\vec{a}_{c4n} = 0 \tag{3.32}$$

$$\vec{a}_{c4t} = 0 \tag{3.33}$$

$$\vec{a}_{c3c4n} = 0 \tag{3.34}$$

$$V_{c3c4} = V_{C3} => Linear\ Piston\ Speed \tag{3.35}$$

$$2 \times |\vec{V}_{c3}| \times w_4 => Coriolis\ Acceleration \tag{3.36}$$

$$\vec{a}_{An} = w_2^2 \times |OA| \tag{3.37}$$

$$\vec{a}_{C3C4t} = w_4^2 \times |AC| \tag{3.38}$$

$$\vec{a}_{c3c4t} = Linear\ acceleration\ of\ the\ piston \tag{3.39}$$

If $\vec{a}_{c3c4t}$ is zero and the piston has a constant speed the dashed lines are going to be representing Coriolis Acceleration and tangential acceleration of point C about point A.

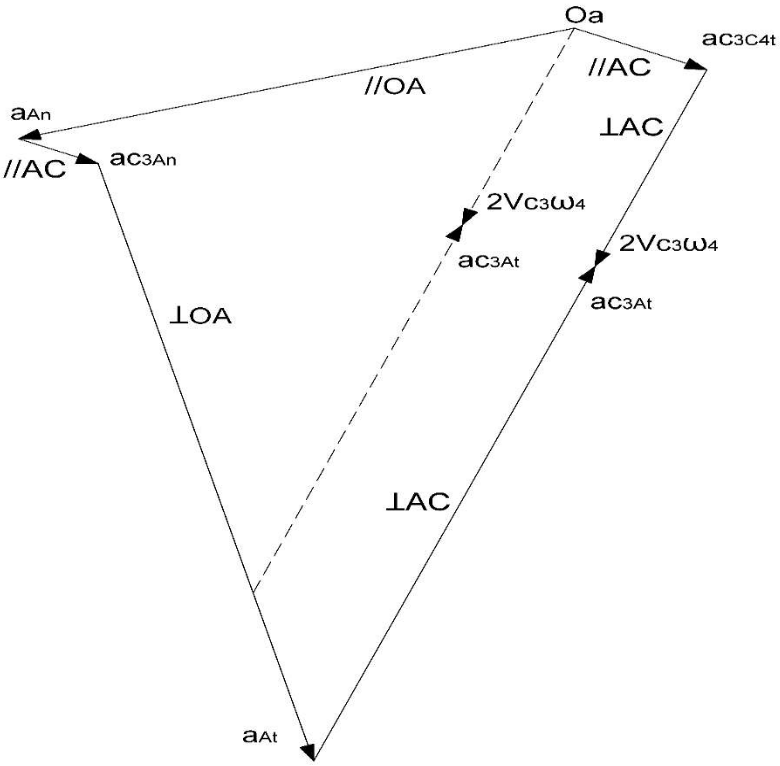

Figure 3.7. Boom Acceleration Analysis

The bucket breakout force of the backhoe loader machine has been calculated with reference to its maximum pump pressure (220 bar). As seen in Figure 3.1, the maximum breakout force that the bucket can apply to the ground in the dynamic analysis starting position is calculated with Eqs. 3.40-3.45 as:

$$P_{pump} = 22000\ kPa \tag{3.40}$$

$$D_{bc} = \emptyset 0.1\ m \tag{3.41}$$

$$F_{bc} = \frac{(\pi \times D_{bc}^2)}{4} \times P \tag{3.42}$$

$$F_{bc} = \frac{(3.14 \times 0.1^2)}{4} \times 22000 \tag{3.43}$$

$$F_{bc} = 172.7(kN) \tag{3.44}$$

$$F_B = \frac{F_{bc} x h_2 x h_4}{h_3 \times h_5} = \frac{172.7x430x246}{345 \times 897} => F_B = 59.05\ kN \tag{3.45}$$

The calculated maximum breakout force is 59.05 kN, which is a quite high value. However, the backhoe loader machine will be able to pull dry sand from a well at full capacity with a force much lower than the calculated maximum shear force. In addition, the scenario is not based on shear force during excavation, as there are vibration and shock analyses underway among the analyses applied.

The digging position of the backhoe design is analyzed and then the critical position determined by dynamic analysis is used in the static analysis model which takes on the role of the main carrier in the backhoe design. The critical position will serve as a reference for the model in each of the static, natural frequency, vibration and shock analyses.

3.1. Backhoe Current Design

The material quality of the parts that make up the Backhoe design group is shown in Table 3.1. Material assignments used in the model are made and the analysis results are examined considering the mechanical properties of the material quality.

Table 3.1. Material Properties

Material	Density (kg/mm³)	Modulus of Elasticity (MPa)	Poisson's Ratio	Yield Strength (MPa)	Tensile Strength (MPa)
S355J2	7800	2.00E+05	0.29	355	630

3.1.1. Transient Structural Mechanical Model for Lifting

The models to be used in dynamic analysis are determined from the physical motions of the backhoe loader machine in real life. Then, the average times for extending and retracting the boom cylinder and stick cylinder are calculated in order to assume constant speed cylinder motion (Lüye, M., 2022). By using the Transient Structural module in Ansys Workbench R18.1 program, a model for dynamic analysis is prepared by taking the time and boundary conditions of the backhoe bucket full capacity dry sand loaded .

The application of the boundary conditions in the Transient Structural module is shown in Table 3.2 where the model is presented in Figure 3.8. A constant load was applied to the inner surface of the bucket in the Y-axis direction and –Y direction, representing the full capacity dry sand load, throughout the analysis period. For the analysis, the boom cylinder is retracted whereas the stick and bucket cylinders are extended.

Table 3.2. Boundary Conditions for Dynamic Analysis

	Rod Displacement (mm)	Time (s)	Force in Bucket (N)	Gravity (mm/s^2)
Rod of boom	600	2	4750	9806.6
Rod of stick	200	3	4750	9806.6
Rod of bucket	280	5	4750	9806.6

As seen in Figure 3.9, the application of the meshing process to the models by applying the “Generate Mesh” process is focused on the parts that will be examined and that will not prevent the force transfer. Mesh criteria are preferred as default so as not to extend the dynamic analysis solution time too much. In Table 3.3, the options selected while creating the mesh for the dynamic analysis model and the quality in the mesh metric criteria are listed.

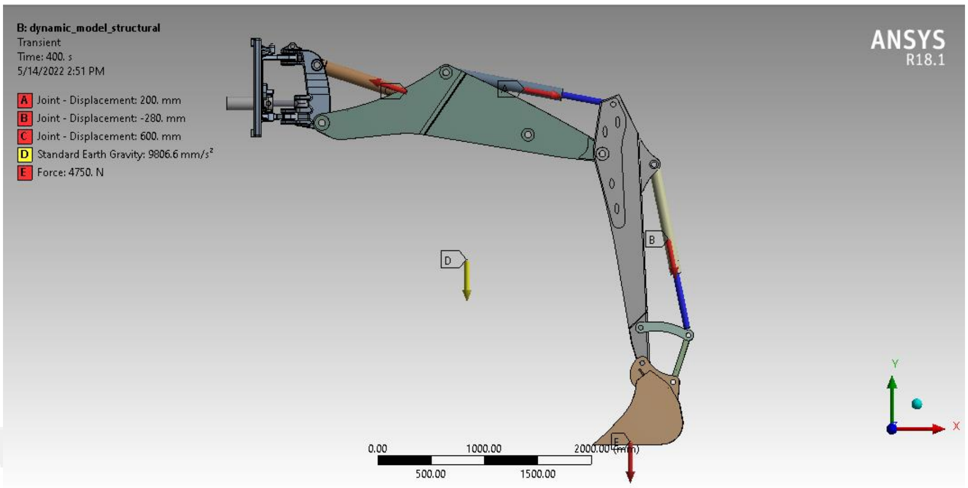

Figure 3.8. Transient Structural Model

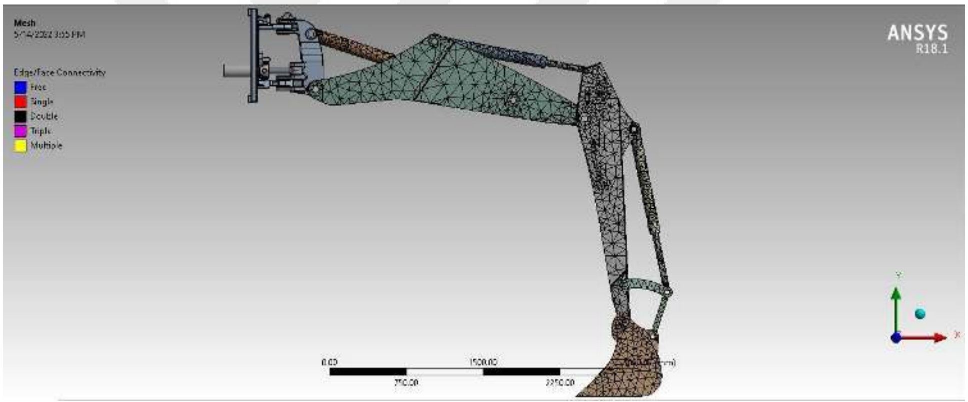

Figure 3.9. Mesh Generation for Transient Structural

Table 3.3 Mesh Quality for Transient Structural Current Design

Mesh Quality	Transient Structural
Physics Preference	Mechanical
Solver Preference	Mechanical APDL
Element Order	Program Controlled
Size Function	Adaptive
Relevance Center	Coarse
Element Size	Default
Nodes Number	178686
Elements Number	105603
Mesh Metric	0.481

3.1.2. Static Structural Mechanical Model for Backhoe Critical Design

With the help of dynamic analysis, the critical position is determined and a model is established in the static structural module with the same boundary conditions in order to examine this position in more detail. As seen in Figure 3.10, the critical position of the backhoe design, which is determined in the dynamic analysis results, is examined in a computer-aided environment with the help of Solidworks program.

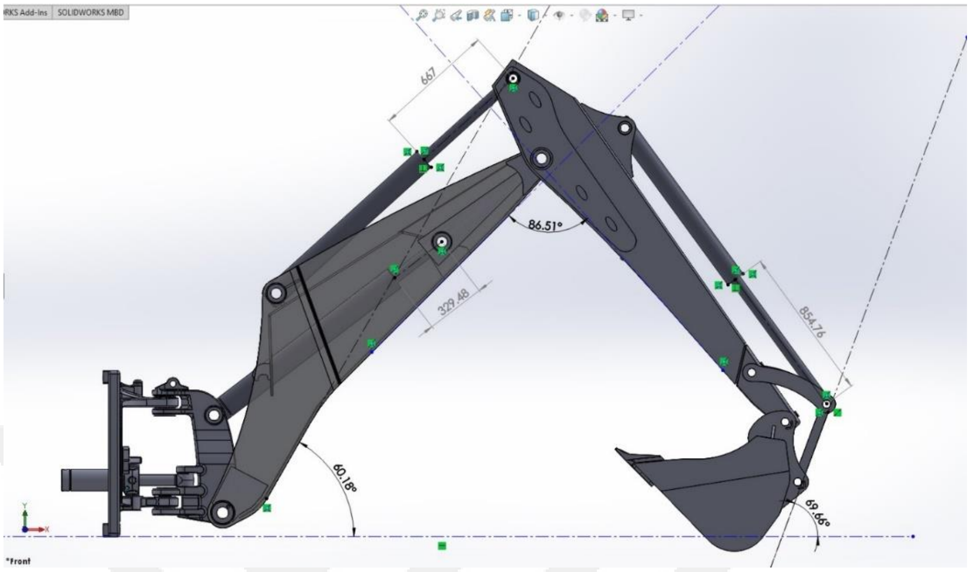

Figure 3.10. Critical Position of Backhoe Design

A model is established for static analysis by reference to the critical position that is determined and the position analysis is made. The simplification of 3D data started with making it ready for analysis in model establishment phase with Shell and beam methods. The sideshift design group, which serves as the base in the backhoe design, is simplified, and the sheetmetal elements, which are widely found in the backhoe design, are transformed into shell elements with the midsurface method. In addition, cylinder and rod parts are considered rigid and converted into beam elements. The moments of inertia of the full capacity dry sand load in the bucket are calculated with the Ansys Workbench mechanical module, and the model is prepared for analysis by defining the point mass inside the bucket.

The simplified analysis model of the backhoe design is expressed in Figure 3.11. The obtained model is used in the static, random vibration and shock analyses to be carried out.

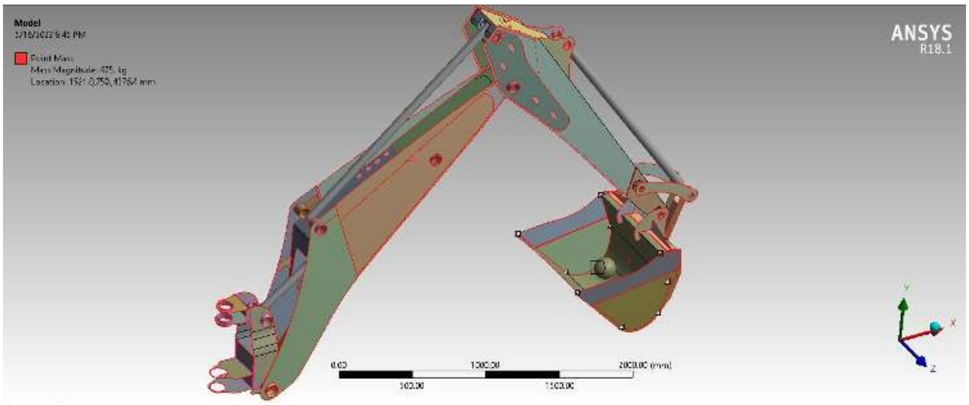

Figure 3.11. Current Model of Backhoe Design

Welded connections between sheetmetals are modeled with bonded contact in the design. By defining a revolute joint to boom, stick and bucket connection points, radial movement is allowed as in reality. Due to the beam elements used to represent the cylinders, a model that can carry a load of backhoe design is established as shown in Figure 3.12.

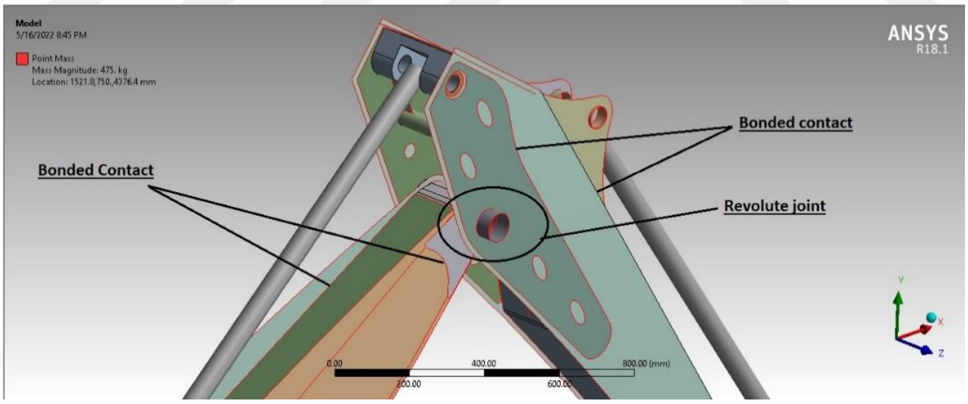

Figure 3.12. Contacts and Joints in Backhoe Design

The mesh of the Backhoe design is expressed in Figures 3.13 and 3.14. The mesh values obtained as a result of the mesh operation are as seen in Table 3.4. Using Shell and beam methods, the average element quality is read as high as 0.923.

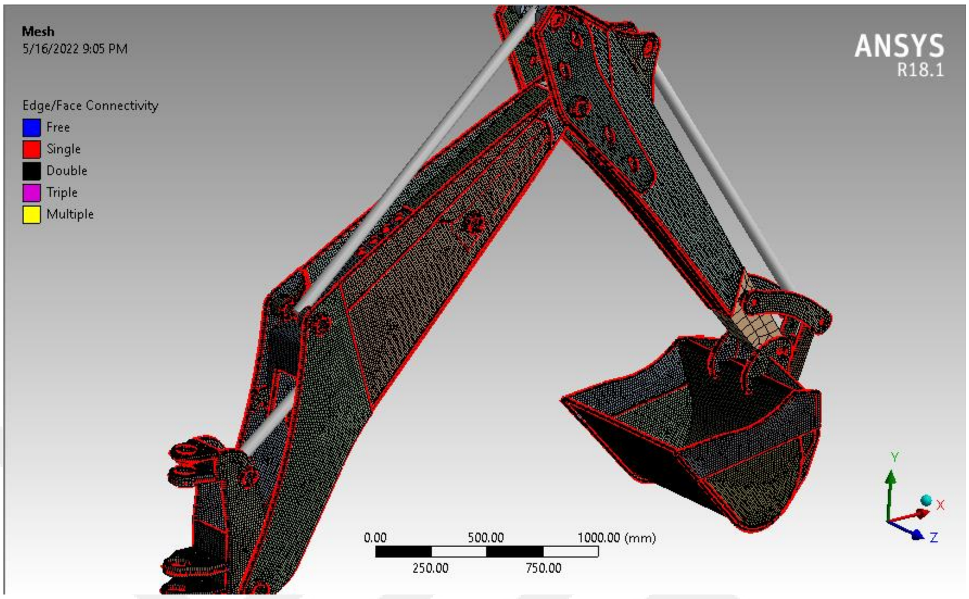

Figure 3.13. Mesh Quality of Backhoe Design

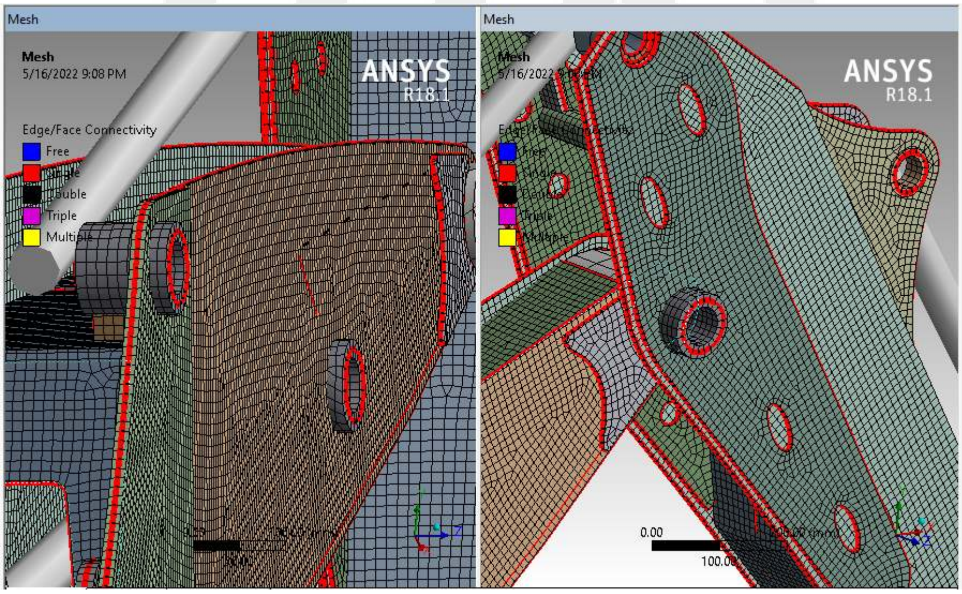

Figure 3.14. Mesh Quality of Backhoe Design

Table 3.4 Mesh Quality for Static Structural Current Design

Mesh Quality	Static Structural
Physics Preference	Mechanical
Solver Preference	Mechanical APDL
Element Order	Program Controlled
Size Function	Adaptive
Relevance Center	Coarse
Element Size	12mm
Nodes Number	86803
Elements Number	75734
Mesh Metric	0.923

The full capacity dry sand load in the bucket design group is defined as the point mass and the information on the point mass is given in Table 3.5. The visual of the point mass is shown in Figure 3.15 and inertia of mass point is calculated by helping of equations 3.45-3.47

$$I_x = m_x \times {r_x}^2 \tag{3.45}$$

$$I_y = m_y \times {r_y}^2 \tag{3.46}$$

$$I_z = m_z \times {r_z}^2 \tag{3.47}$$

Table 3.5 Point Mass Information

Mass	475 kg
I_x	19975589 $kgxmm^2$
I_y	31441680 $kgxmm^2$
I_z	36909368 $kgxmm^2$

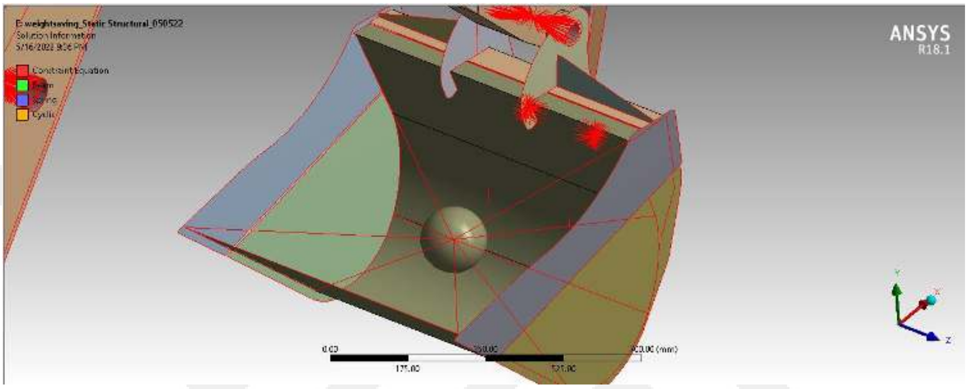

Figure 3.15. Point Mass in Bucket Design

In Table 3.6, the weight and thickness information of the boom wall plate and boom traverse plate that make up the current boom design are given. The lightening work is aimed at these 2 parts with a focus on boom design.

Table 3.6 Part Properties of Boom Design

Part	Material Quality	Thickness (mm)	Weight (kg)
Boom Main Wall	S355J2	20	66.56
Boom Top Travers	S355J2	10	21.61

There are 2 pieces of main boom wall sheet, right and left, in a boom design group as shown in Figure 3.16. The upper traverse sheet, on the other hand, has 1 piece between the two wall sheets (Figure 3.17). The stresses on the parts, the colored image of the stress, the thicknesses they have and the material quality have been effective in the selection of the parts to be focused on in the lightening studies.

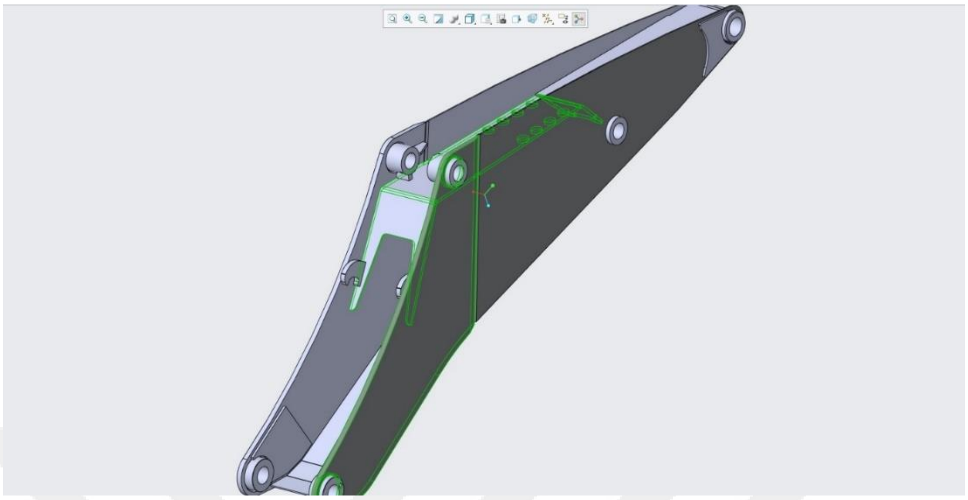

Figure 3.16. Current Boom Design

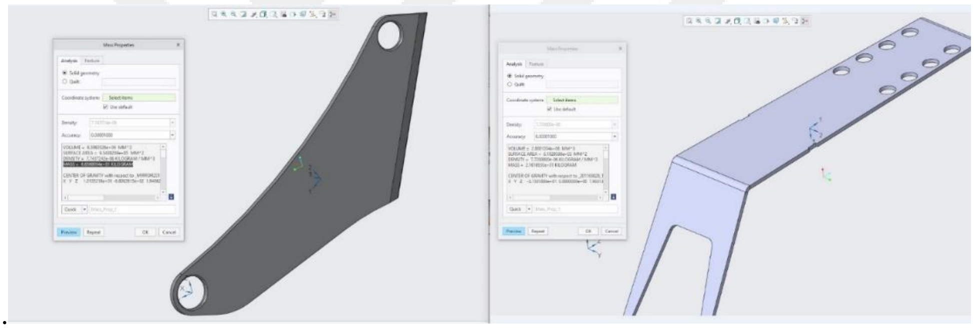

Figure 3.17. Parts of Current Boom Design

With the static analysis based on the critical position, the backhoe design is structurally examined. The determination of the design group and parts to be focused on in the reducing weight study is made in a computer-aided environment. These procedures have a guiding effect on weight reducing efforts.

The main boom wall plate and the upper traverse plate are each selected from S355J2 material, which is 4 mm thinner but with the same material quality. The backhoe design is updated accordingly. With the changes made, the current weights of the main boom sheets and the upper traverse sheet are determined in a computer-aided environment using the Solidworks program. As can be seen in Figure 3.18, the current main boom sheet thickness is 16 mm and its weight is 54.84 kg whereas the current upper traverse sheet thickness is 6 mm and its weight is 13.06 kg. The current design weight data of the parts are listed in Table 3.6.

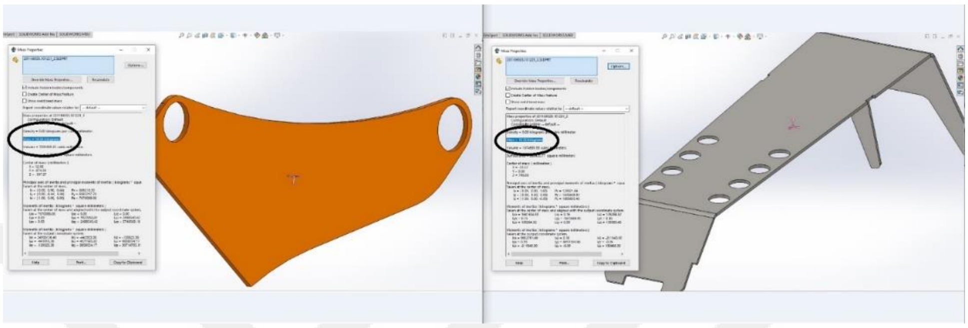

Figure 3.18. New Design Weight of Parts

Table 3.7 Part Properties of New Parts in Boom Design

Part	Current Weight (kg)	New Weight (kg)	Number	Weight Saving (kg)
Boom Main Wall	66.56	54.84	2	23.45
Boom Top Travers	21.61	13.06	1	8.55
Total				32.00

As a result of the determinations made in a computer-supported environment, as can be seen in table 3.7, the total weight reduction is calculated as 32 kg for sheets with S355J2 material quality. The 32 kg lighter backhoe design is in the critical position (See Figure 3.18) will be subjected to static, modal, random vibration and shock analyzes, respectively, according to military standards (MIL-STD-810). Thus, the effect of the weight reduction effort on the strength of the backhoe design will be examined.

3.2. Backhoe New Design

3.2.1. Static Structural Model for Backhoe New Design

The lightweight backhoe design is modeled with the same boundary conditions as performed in the preliminary study. The model installed with the bucket at full capacity in the critical position determined by the help of dynamic analysis is shown visually in Figure 3.19.

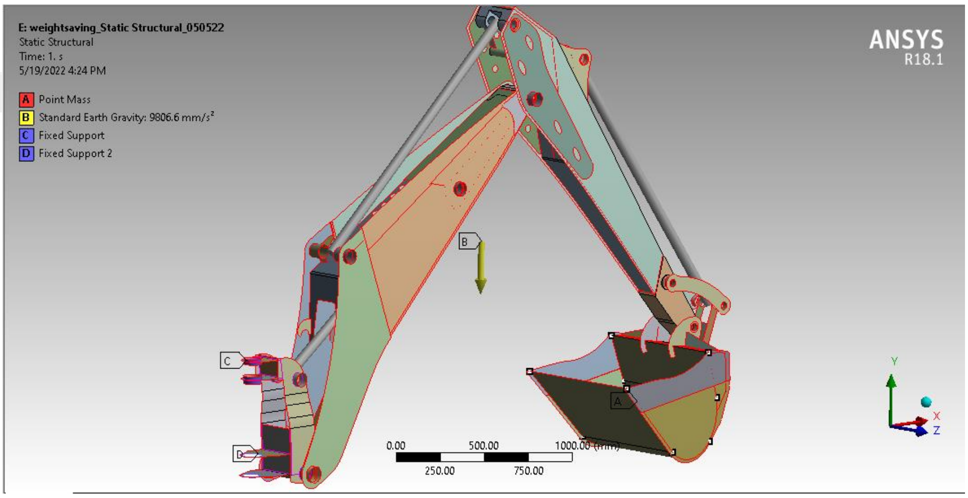

Figure 3.19. Static Structural Model for New Design of Backhoe

The load in the bucket is modeled as a point mass and is the same weight as in the preliminary study (See. Figure 3.15). Connection structures between sheetmetal parts and joints defined between design groups are the same as expressed in Figure 3.12. Mesh properties of the backhoe model are also determined to be the same as the mesh properties in the preliminary study in order to compare the results properly. Information about mesh properties and quality is as stated in Figure 3.13, Figure 3.14 and Table 3.4.

Table 3.8 Part Thickness of Boom Design

Part	Current Thickness (mm)	New Thickness (mm)
Boom Main Wall	20	16
Boom Top Travers	10	6

3.2.2. Modal Analysis Model for Backhoe New Design

The modal analysis model is established with reference to the static structural model. The backhoe design with modal analysis is made to detect natural frequencies and observe the effective mass ratio participation rate under full load in the critical position. In this way, we can perform vibration and shock analysis that are healthier and that we will be sure of the results.

In model analysis, an analysis model is established with 30 modes. The natural frequencies of the backhoe design are determined in each mode number. "Analysis setting" information for modal analysis is expressed in Figure 3.20.

3.2.3. Random Vibration Analysis Model for Backhoe New Design

The model used in the random vibration module is the same as the static structural module used in the lightweight backhoe design (See Figure 3.19). In order to examine the model at different angles, another image is shared in Figure 3.21.

Details of "Analysis Settings"	
Options	
Max Modes to Find	30
Limit Search to Range	No
Spin Softening	Program Controlled
Solver Controls	
Damped	No
Solver Type	Direct
Rotordynamics Controls	
Output Controls	
Stress	Yes
Strain	Yes
Nodal Forces	Constrained Nodes
Calculate Reactions	Yes
Store Modal Results	Program Controlled
General Miscellaneous	No
Analysis Data Management	

Figure 3.20. Modal Analysis Setting

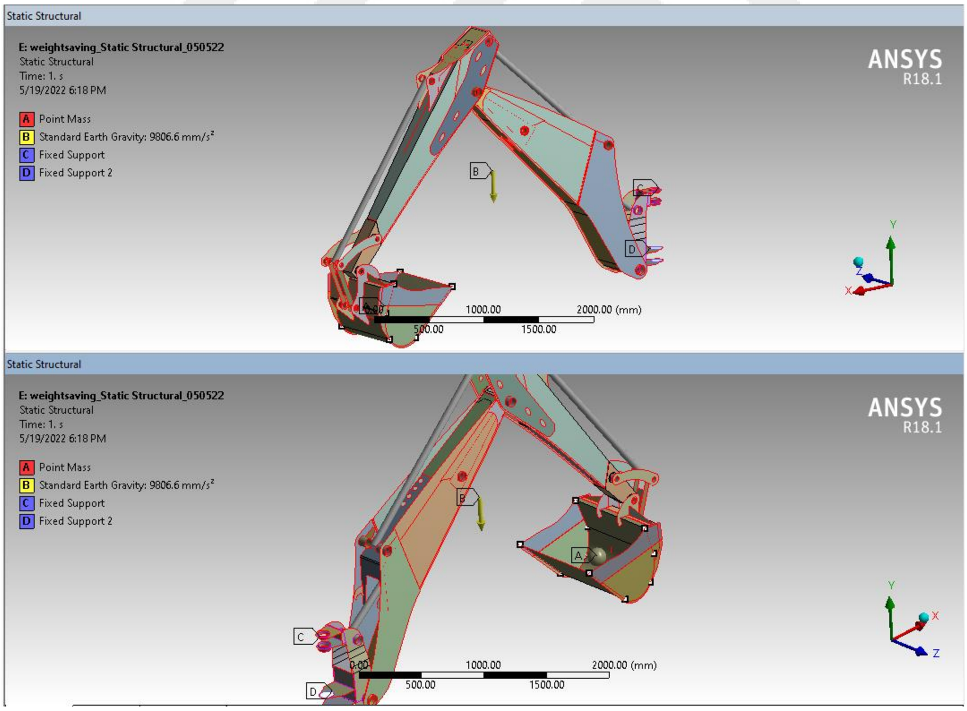

Figure 3.21. Model of Backhoe Design

Backhoe design is fixed by making fixed support from the sideshift part. Connections between other assembly groups (boom, stick, bucket) are provided with revolute joint and beam elements.

Boundary conditions of random vibration analysis are outlined in Table 3.9. Vibration loads are added to the boundary conditions by importing the data determined by previous tests for land transportation on all 3 axes to the Ansys Workbench program. Random vibration loads are used with reference to the military standard below. In line with the boundary conditions applied for vibration analysis, the damage values on the structure will be examined. Evaluations are made by taking into account the 'Steinberg' criterion. Steinberg's theorem interprets the damage caused by loads applied to a structure over a period of time and assumes it to be safe if it is below 1. This theorem is available for damage calculations in FEM programs.

Based on random vibration loading of MIL-STD-810, Method 514.7, Category 4, Table 514.7C-I and Figure 514.7C-2 (Common carrier, US highway truck vibration exposure) the vibration profile is listed in Table 3.9 with a loading time of 3600 seconds.

Table 3.9. Highway Vibration Profile

HIGHWAY X		HIGHWAY Y		HIGHWAY Z	
Frequency (Hz)	G^2/HZ	Frequency (Hz)	G^2/HZ	Frequency (Hz)	G^2/HZ
5	0.1759	5	9.98E-02	5	4.14E-02
8	0.512	7	7.99E-02	7	3.90E-02
9.3808	0.18383	9	0.1115	8	5.76E-02
11	6.60E-02	10	5.77E-02	9	4.30E-02
12	5.85E-02	14	2.94E-02	10	2.93E-02
13	3.48E-02	15	6.51E-02	13	2.21E-02
15	0.1441	16	6.46E-02	15	5.85E-02
16	0.1237	17	4.36E-02	16	5.85E-02
17.889	5.46E-02	18	3.93E-02	16.971	2.42E-02
20	2.41E-02	19	6.22E-02	18	1.00E-02
23	5.36E-02	21.354	2.49E-02	20	9.90E-03
24.454	2.58E-02	24	1.00E-02	23	4.52E-02
26	1.24E-02	37	4.50E-03	23.979	2.23E-02
27	1.18E-02	38	6.50E-03	25	1.10E-02
30	3.31E-02	44	3.30E-03	35	3.60E-03
31.937	1.69E-02	55	2.40E-03	37	9.80E-03

34	8.60E-03	57	4.20E-03	40	4.00E-03
39	3.47E-02	59	1.90E-03	41	4.40E-03
40.951	1.59E-02	76	1.20E-03	45	2.30E-03
43	7.30E-03	79	2.10E-03	47	4.70E-03
45	1.41E-02	83	1.00E-03	50	1.60E-03
49	8.40E-03	114	6.00E-04	54	1.70E-03
52	8.90E-03	135	1.70E-03	64	1.00E-03
57	4.50E-03	142	1.00E-03	69	3.00E-03
67	1.60E-02	158	1.80E-03	72.89	1.45E-03
73.212	7.69E-03	185	1.00E-03	77	7.00E-04
80	3.70E-03	191	7.00E-04	85	1.50E-03
90	7.70E-03	206	8.00E-04	90	1.20E-03
93	5.30E-03	273	3.50E-03	97	1.50E-03
98	6.50E-03	300	1.60E-03	104	3.60E-03
99	6.30E-03	364	7.40E-03	114	4.00E-03
111	4.60E-03	374	2.20E-03	122	1.50E-03
123	6.90E-03	395	5.10E-03	132	1.30E-03
128	5.50E-03	444.41	2.47E-03	206	3.30E-03
164	3.10E-03	500	1.20E-03	225.57	8.64E-03
172	3.50E-03			247	2.26E-02
215	1.33E-02			251.95	9.63E-03
264	5.60E-03			257	4.10E-03
276	9.60E-03			264	5.40E-03
292	3.20E-03			276	4.00E-03
348	4.40E-03			303	7.30E-03
417	3.10E-03			332	9.20E-03
456.62	1.57E-03			353	1.72E-02
500	8.00E-04			382	7.10E-03
				428	1.57E-02
				462.6	5.01E-03
				500	1.60E-03

Vibration profiles for highways expressed in Table 3.9 are imported as boundary conditions of the models established for each of the X, Y and Z axes in the Random Vibration module in the Ansys Workbench program.

3.2.3.1. Random Vibration Boundary Conditions for Land Transverse

Vibration loads expressed for the X-axis in the Military Standard, that is, the transverse vibration loads, are loaded in the +Z direction in the Z axis direction, taking into account the coordinate system in the analysis model. Thus, the shock loads expressed in the military standard in the transverse direction are integrated into the model coordinate system and the model with the Land Transverse title is established in the Random Vibration module. The graphic image of the standard vibration load profiles loaded on the model is shown in Figure 3.22.

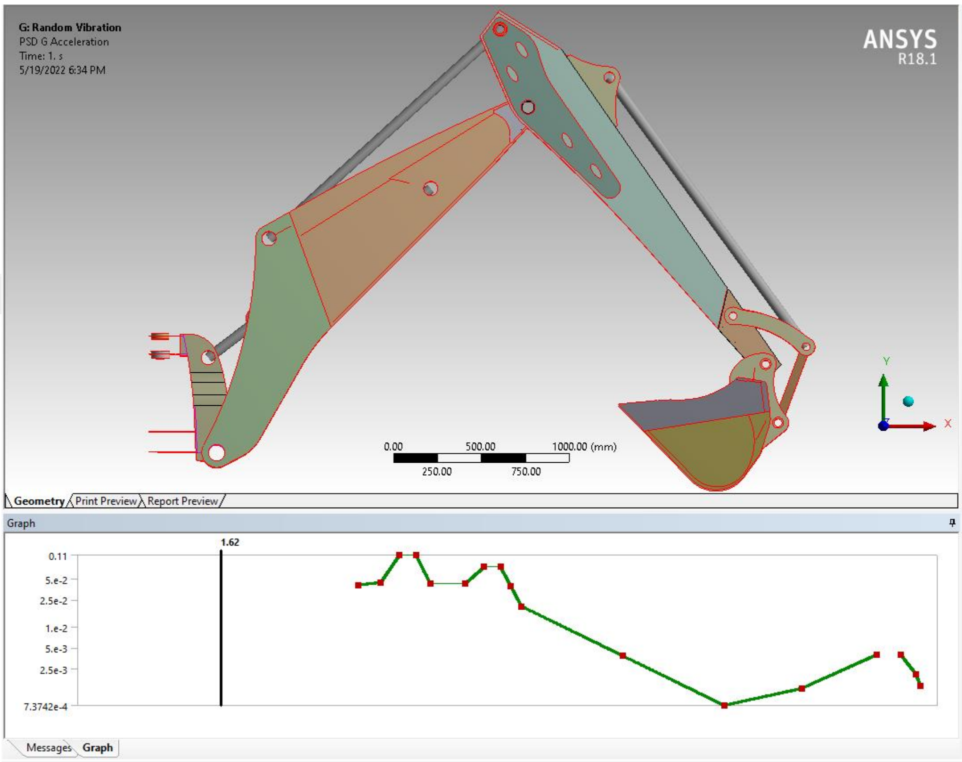

Figure 3.22. Land Transverse Vibration Force

3.2.3.2. Random Vibration Boundary Conditions for Land Longitudinal

Vibration loads expressed for the Y-axis in the Military Standard, that is, longitudinal vibration loads, are loaded in the +X direction in the X-axis direction, taking into account the coordinate system in the analysis model. Thus, the shock loads expressed in the military standard in the longitudinal direction are integrated into the model coordinate system and the Land Longitudinal model is established in the Random Vibration module. The graphic image of the standard vibration load profiles loaded on the model is shown in Figure 3.23.

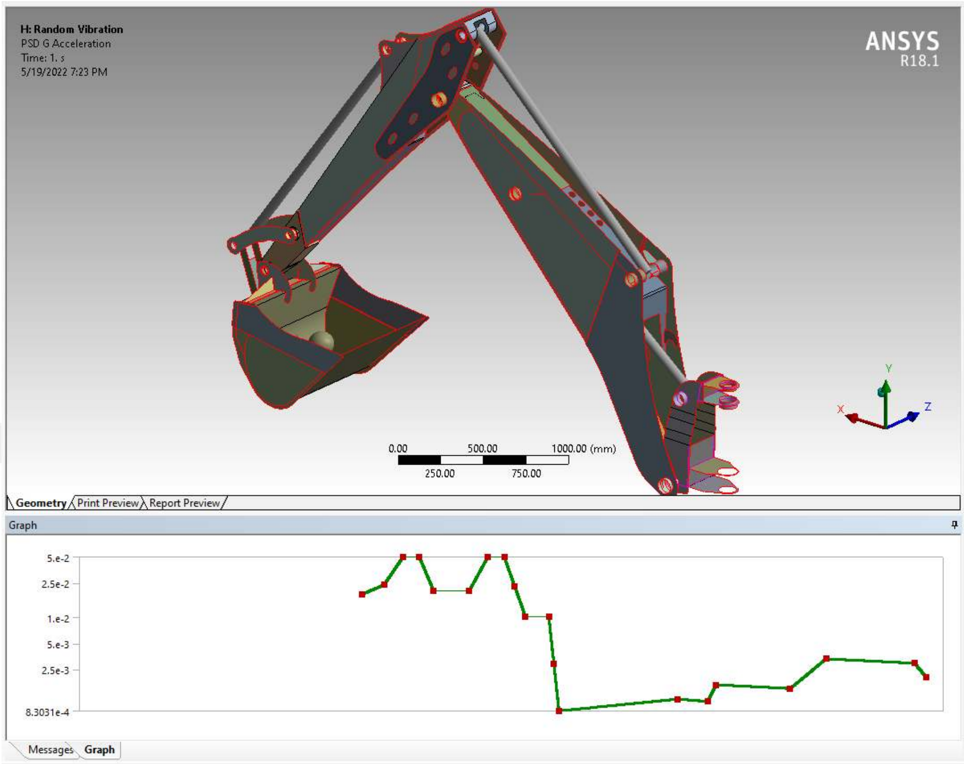

Figure 3.23. Land Longitudinal Vibration Force

3.2.3.3. Random Vibration Boundary Conditions for Land Vertical

Vibration loads expressed for the Z axis in the Military Standard, namely vertical vibration loads, are loaded in the +Y direction in the Y axis direction, taking into account the coordinate system in the analysis model. Thus, the shock loads expressed in the vertical direction in the military standard are integrated into the model coordinate system and the model with the Land Vertical title is established in the Random Vibration module. The graphic image of the standard vibration load profiles loaded on the model is shown in Figure 3.24.

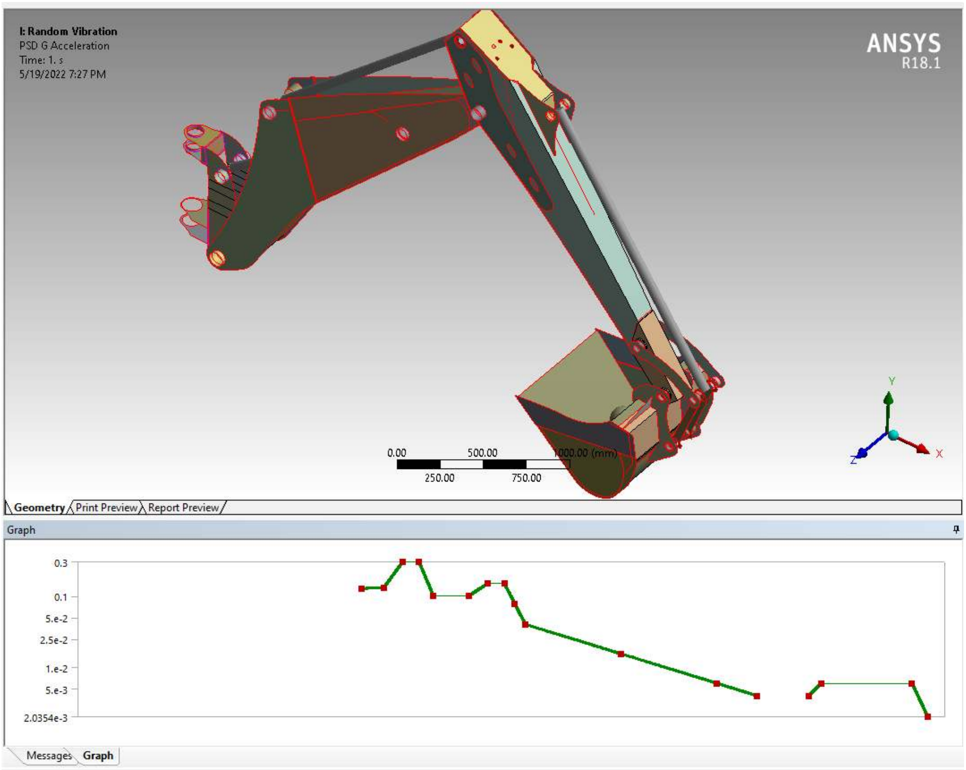

Figure 3.24. Land Vertical Vibration Force

3.2.4. Shock Anlysis for Backhoe New Design

Dynamic-based Transient Structural module in Ansys Workbench program is used for shock analysis. The new backhoe design model is used in the shock analysis as previously stated (See Figure 3.19). Shock loads determined according to military standards are imported into the model in the form of sawtooth (terminal). Shock loads are used according to the reference given below.

- MIL-STD-810, Method 516.7, Table 516.7-VI, in 15.2g 5 ms sawtooth (terminal) waveform

3.2.4.1. Shock Analysis Transverse

Shock loads are applied in sawtooth shape with a size of 15.2g. In order to perform shock analysis in the transverse direction, the shock load is loaded in the +Z direction in the Z direction, taking the coordinate system of the model as a reference. As can be seen in Figure 3.25, the model is set up to apply a shock load that will affect the entire design in the Z direction in a small time interval such as 5 ms with sudden acceleration.

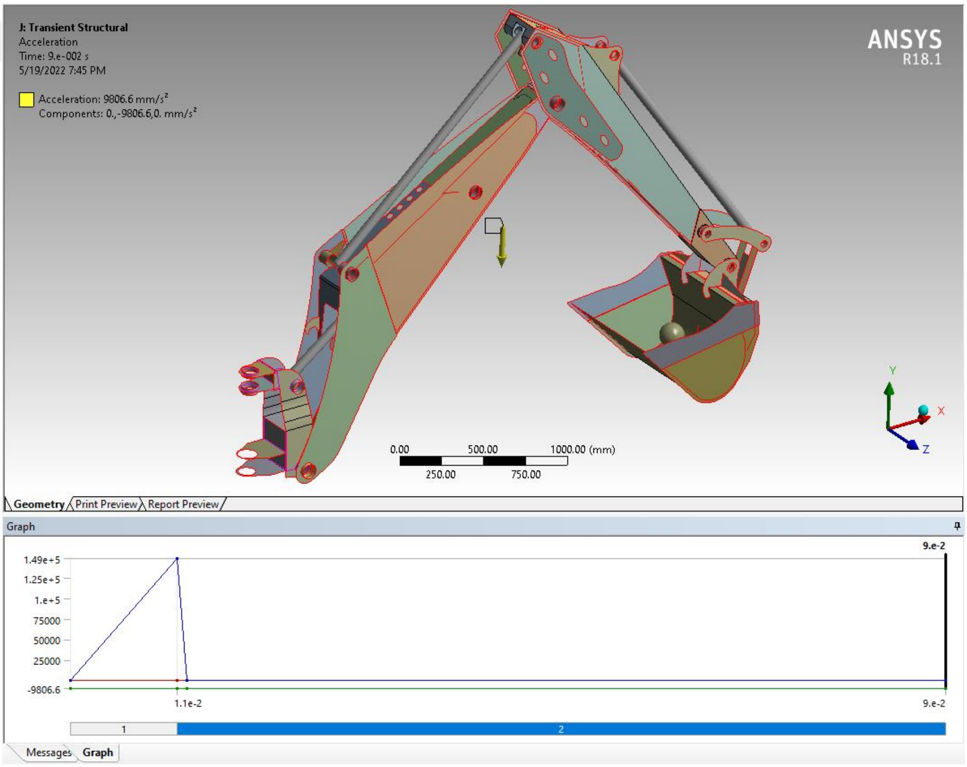

Figure 3.25. Transient Analysis Transverse Shock

3.2.4.2. Shock Analysis Longitudinal

Shock loads are applied in sawtooth shape with a size of 15.2g. In order to perform shock analysis in the longitudinal direction, the shock load is loaded in the X direction + X direction, taking the coordinate system of the model as a reference.

In order to apply a shock load that will affect the entire design in the X direction in a small time interval such as 5 ms with sudden acceleration, the model with the shock load direction X, like the model expressed in Figure 3.25, is established.

3.2.4.3. Shock Analysis Vertical

Shock loads are applied in sawtooth shape with a size of 15.2g. In order to perform shock analysis in the vertical direction, the shock load is loaded in the +Y direction in the Y direction, taking the coordinate system of the model as a reference. In order to apply a shock load that will affect the entire design in the Y direction in a small time interval such as 5 ms with sudden acceleration, a model with the shock load direction Y, like the model expressed in Figure 3.25, is established.

4. RESULTS AND DISCUSSION

The results of dynamic, static, modal, shock and vibration analyses performed respectively for the lightweight backhoe design were examined and interpreted with an engineering approach. The dynamic analysis results for the critical position determination and then the model established by taking the critical position as a reference, with the help of static analysis, it was determined which regions or parts should be concentrated in the weight reduction studies. The weight reduction effort has been done in the backhoe design. The new backhoe design consisting of thinner sheets has been remodeled in the same boundary conditions in the critical position. By applying static, modal, vibration and shock analyses to the lightweight backhoe design, respectively, the attenuation is examined structurally on the boom design.

Equivalent stresses, deformations and damage values were checked in this section. The resulting stresses were compared with the yield strengths of the relevant materials. Vibration analysis results in military standard conditions (See Fig. MIL-STD-810G) were examined to check whether damage values were above 1.

4.1. Backhoe Current Design Results

4.1.1. Transient Structural Analysis Result for Current Backhoe Design

By examining the results of the dynamic analysis made in the Transient Structure module, the time-dependent movement of the backhoe design was examined. With the help of the animations obtained, the time and location where the design was exposed to the most equivalent stress in the bucket full load condition were determined. Structural analysis results were examined with a focus on the boom design, which acted as the main carrier, and it was aimed to carry out the weight reduction effort in this design group.

As a result of the dynamic analysis, the maximum equivalent stress was determined as 51.874 MPa, which is seen in Figure 4.1. The critical position at which the maximum stress was read has been detected. It has been determined that the region where the stress was the highest occurred in the sheet that acted as the lower cross member between the boom wall sheets that make up the boom design, as seen in figure 4.2.

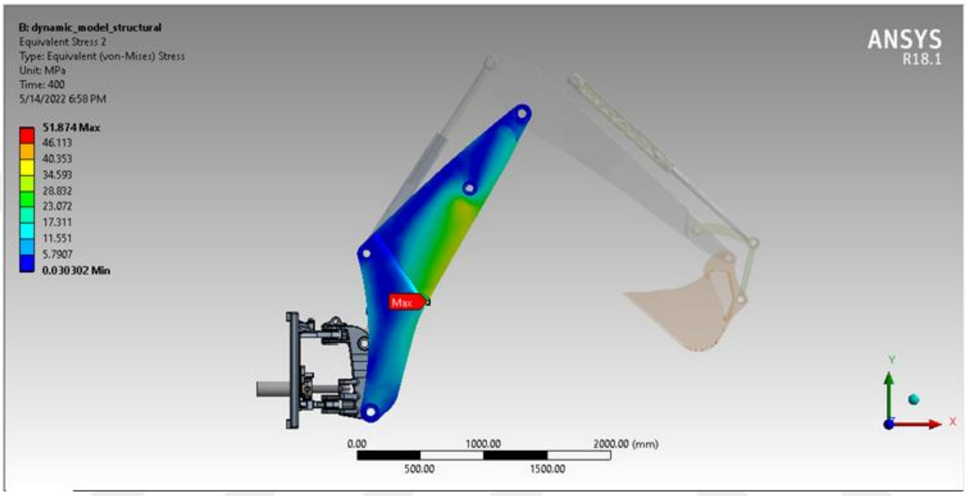

Figure 4.1Transient Structural Maximum Stress Over Time

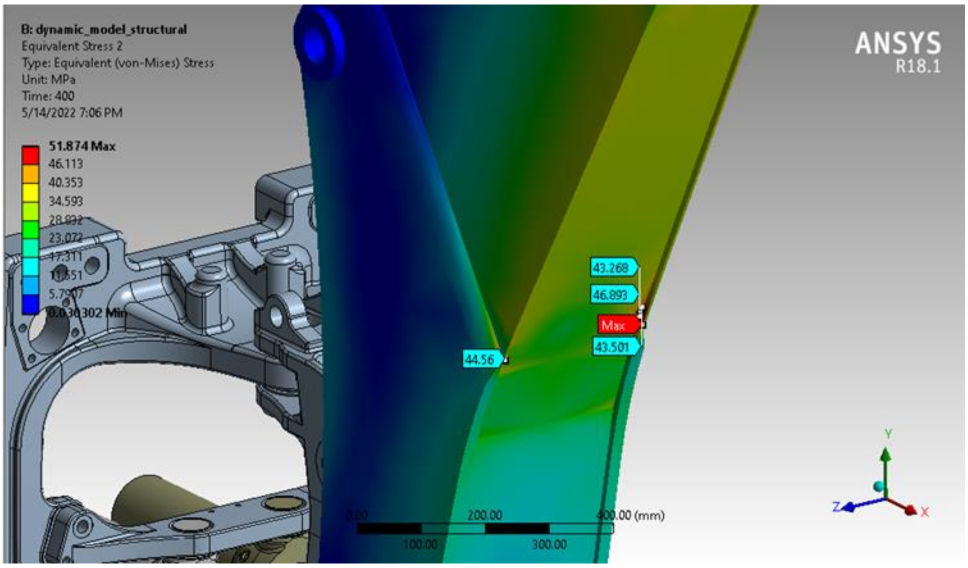

Figure 4.2. Area of Maximum Stress Over Time

4.1.2. Static Structural Analysis Results for Backhoe Current Design

Static analysis results for the existing backhoe design in the Static Structural module were examined. The maximum equivalent stress result of the backhoe design at the critical position was read as 46.75 MPa as seen in Figure 4.3. It has been determined that the highest stress was on the stick design group, but the backhoe design, which was made of sheets with S355J2 material quality, remained in the safety zone under operating conditions.

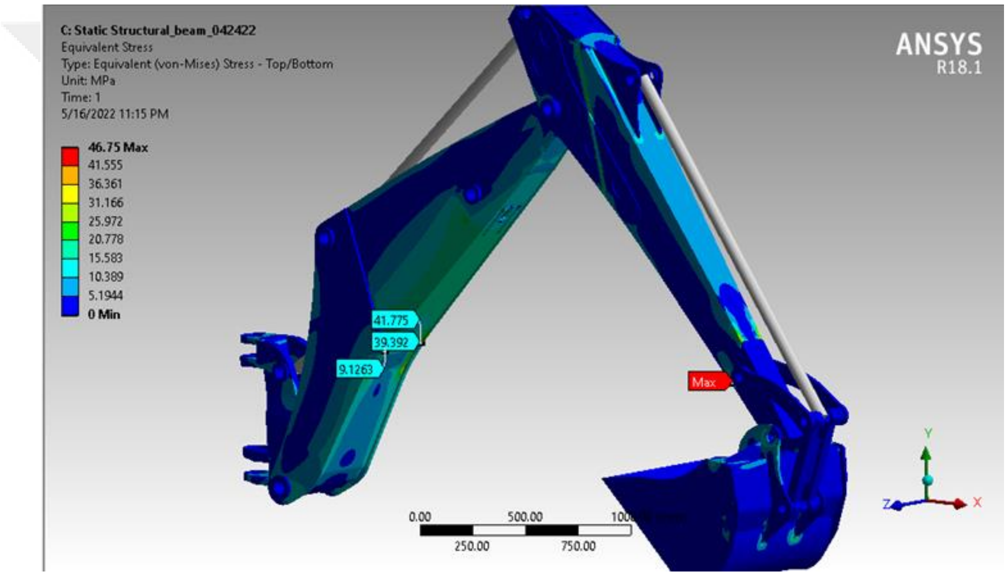

Figure 4.3. Maximum Equivalent Stress of Backhoe Design

It has been determined that another region following the maximum equivalent stress occurred on the boom group. As seen in Figure 4.4 on the boom group, the maximum equivalent stress was read as 43.601 MPa.

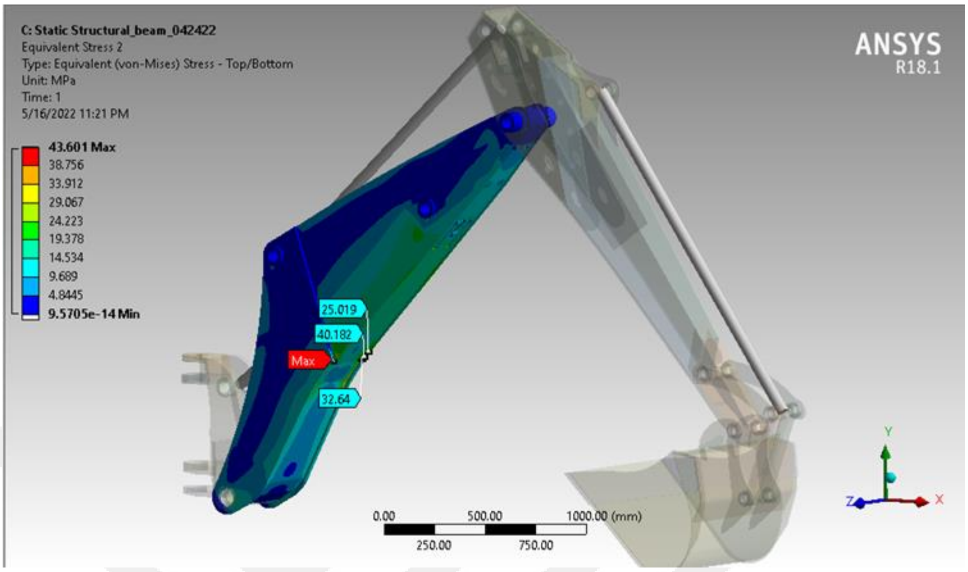

Figure 4.4. Maximum Equivalent Stress of Boom Design

It has been observed that the peak stresses on the boom group at the critical position were similar to the region in the dynamic analysis (See Fig. Figure 4.2). As a result of the examinations made on the existing backhoe design, it was decided that the weight reduction efforts should be directed to the parts where the stresses were not severe on the boom design group. Boom wall sheets and boom traverse sheet thicknesses, which were in the boom design group and had S355J2 material quality, were determined and it was aimed to design a lighter backhoe with similar strength by reducing the thickness of these parts.

The weights of the boom wall sheet and boom traverse sheet parts calculated based on mass volume formula as given in Eq. (4.1) were determined in computer aided environment of Solidworks program. The boom design and parts of it are shown in Figures 4.5 and 4.6. The thickness and weight information of the parts in the current design are given in Table 4.1.

$$m = d \times v \tag{4.1}$$

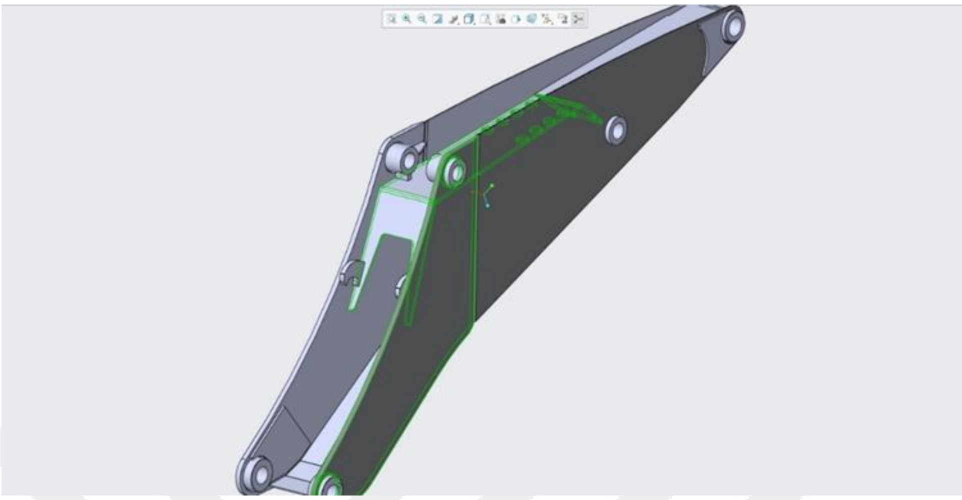

Figure 4.5. Current Boom Design

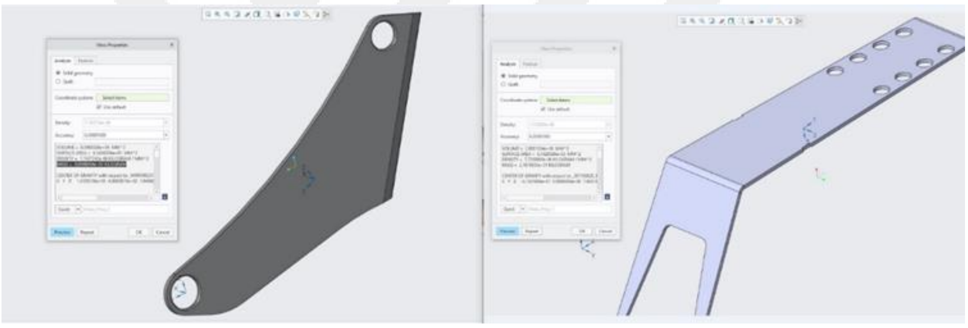

Figure 4.6. Parts of Current Boom Design

Table 4.1 Part Properties of Boom Design

Part	Material Quality	Thickness (mm)	Weight (kg)
Boom Main Wall	S355J2	20	66.56
Boom Top Travers	S355J2	10	21.61

There are 2 pieces of main boom wall sheet, right and left, in a boom design group. The upper traverse sheet, on the other hand, has 1 piece between the two wall sheets. The stresses on the parts, the colored image of the stress, the thicknesses they have and the material quality have been effective in the selection of the parts to be focused on in the weight reduction studies.

4.2. Backhoe New Design Results

4.2.1. Structural Analysis Results for New Backhoe Design

When the lightened backhoe design analysis results are examined, it is seen in Figure 4.7 that the highest equivalent stress was determined as 46.336 MPa. The determined maximum equivalent stress is considerably lower than the yield strength of the S355J2 material that is utilized in the design. High stresses, as found out in dynamic analysis (See Fig. Figure 4.1) has been found to occur at the junction of the boom wall sheets and the boom lower cross member sheet. The regions where the stresses are intense are given in Figure 4.8 in detail. As a result of the examinations, it has been determined that the lightweight backhoe design is statically safe under the boundary conditions specified in Figure 3.12.

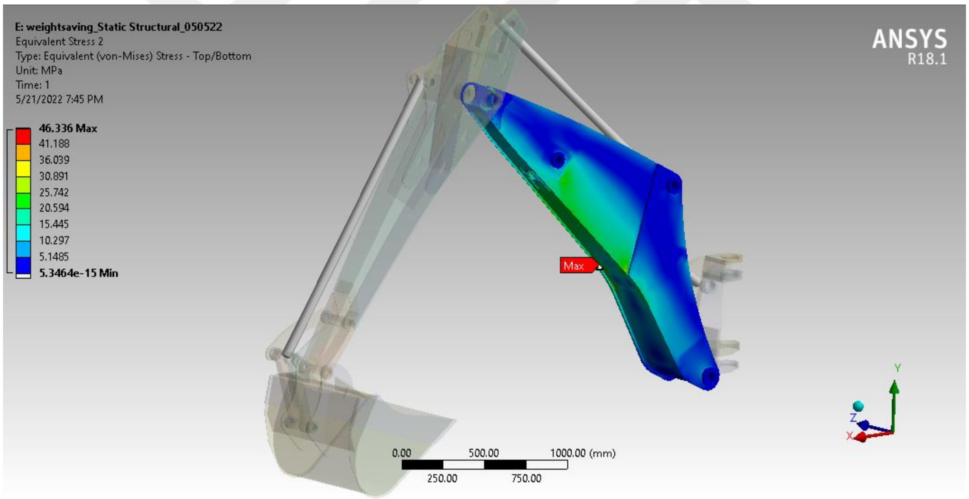

Figure 4.7Static Structural Analysis Results for New Design

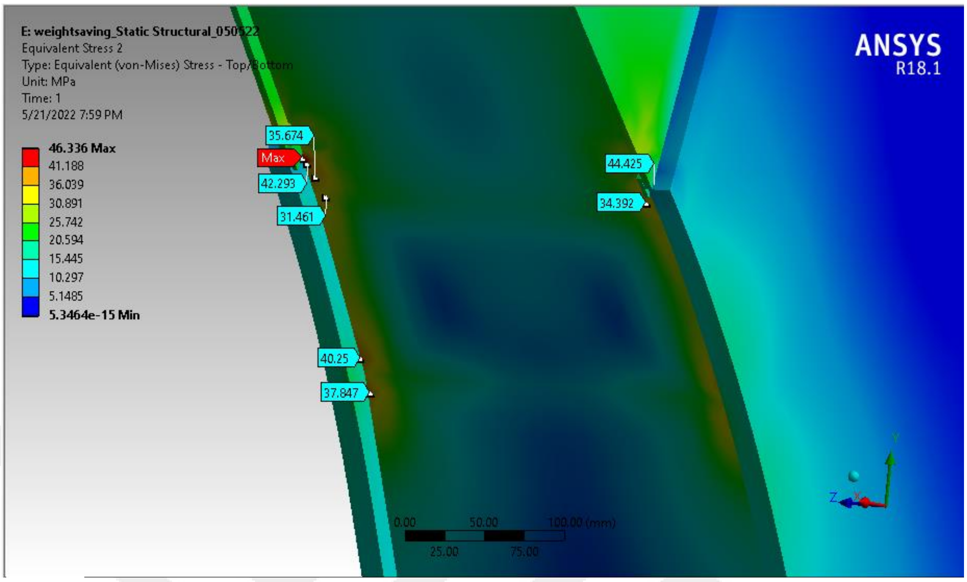

Figure 4.8. Static Structural Analysis Results for High Stress Area

4.2.2. Modal Analysis Results for New Backhoe Design

Color images of the frequency modes formed in line with the boundary conditions applied in the modal analysis are shown in Figure 4.9, Figure 4.10, Figure 4.11 and Figure 4.12. Figure images have been recorded with bigger scales from the Ansys Workbench program in order to be able to make a better analysis. Mass participation rates of the modes are given in Table 4.2. Table of the frequency and mass participation rates obtained for 30 modes are expressed in a simplified form. The fact that the total mass participation ratio is equal to 1 is important for the complete examination of the design in the vibration and shock analyses to be made.

When the cumulative effective mass ratio table is examined, it has been determined that the parts that make up the backhoe design have a high mass participation under the modeled boundary conditions. A large ratio means that vibration and shock loads will affect the entire design highly and the analysis results will be reliable.

Table 4.2. Cumulative Effective Mass Ratio

Mode	Frequency (Hz)	X Direction	Y Direction	Z Direction	X Rotation	Y Rotation	Z Rotation
1	6.0541	4.15E-06	9.89E-09	0.65235	2.4E-02	7.7E-02	4.3E-07
2	7.5945	2.42E-02	0.59498	0.65235	0.55524	9.7E-02	0.42337
3	11.322	0.36064	0.64428	0.65236	0.59879	0.40308	0.42359
4	19.714	0.7912	0.69605	0.65236	0.64446	0.79598	0.761
5	21.198	0.7912	0.69605	0.76737	0.68375	0.79934	0.761
10	95.007	0.79194	0.69606	0.97744	0.72943	0.80794	0.76135
15	128.6	0.87489	0.69774	0.97762	0.73115	0.8832	0.79182
20	158.55	0.92984	0.71247	0.98086	0.74424	0.9343	0.80594
21	160.06	0.93038	0.71295	0.98087	0.74469	0.93478	0.80649
22	161.71	0.9304	0.71295	0.98097	0.74469	0.93478	0.8065
23	165.75	0.9304	0.71295	0.98097	0.74469	0.93478	0.8065
24	182.76	0.93041	0.71296	0.98097	0.7447	0.93479	0.80651
25	189.19	0.93041	0.71306	0.98939	0.74513	0.93516	0.80656
26	198.15	0.93299	0.72078	0.98949	0.75179	0.93773	0.81209
27	201.75	0.95331	0.78886	0.99029	0.81063	0.95804	0.85986
28	204.59	0.95487	0.79471	0.99076	0.81536	0.95976	0.86383
29	209.09	0.98128	0.90447	0.99621	0.9207	0.97903	0.93771
30	216.68	1	1	1	1	1	1

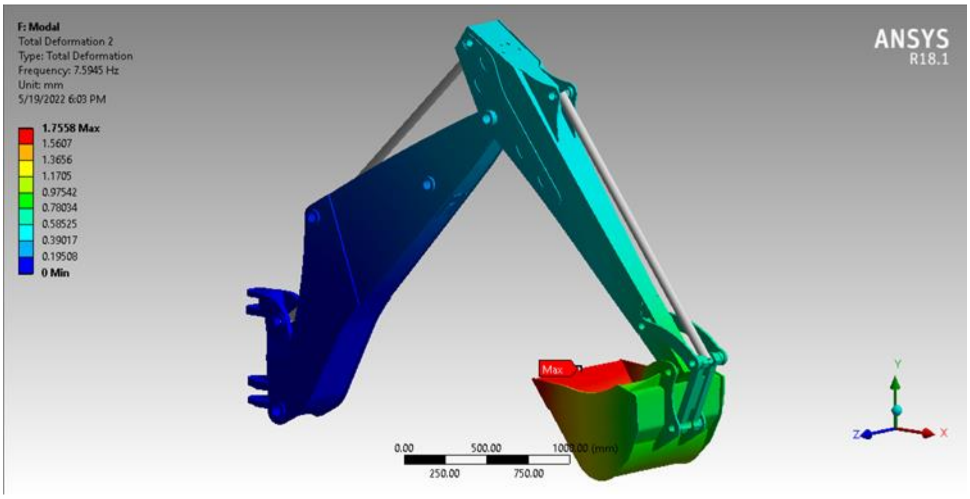

Figure 4.9. Modal Analysis Result On Mode 2

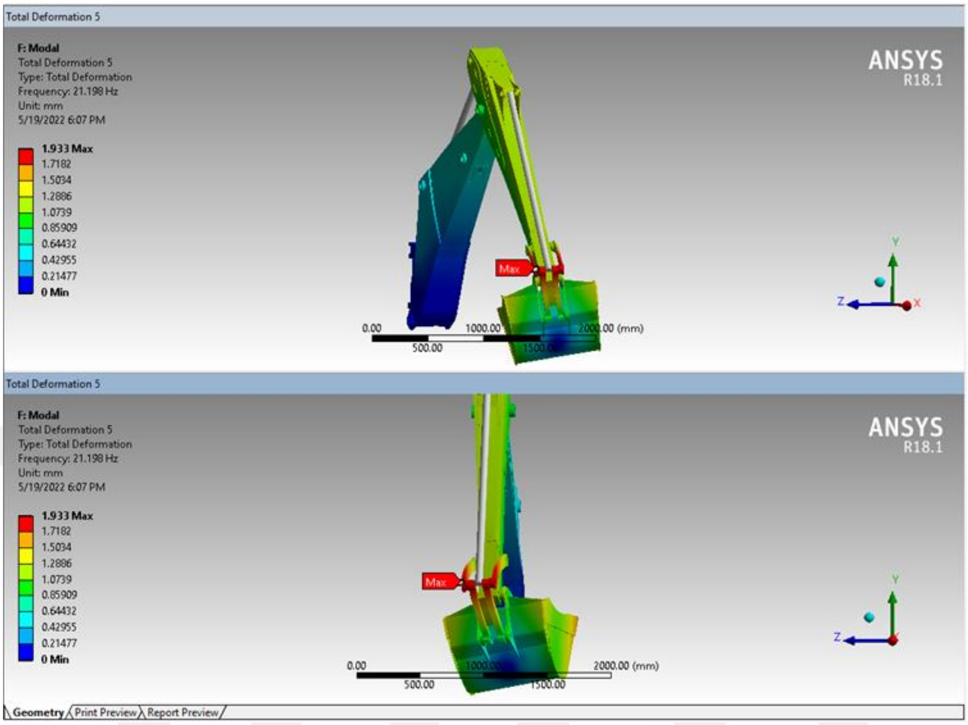

Figure 4.10. Modal Analysis Result On Mode 5

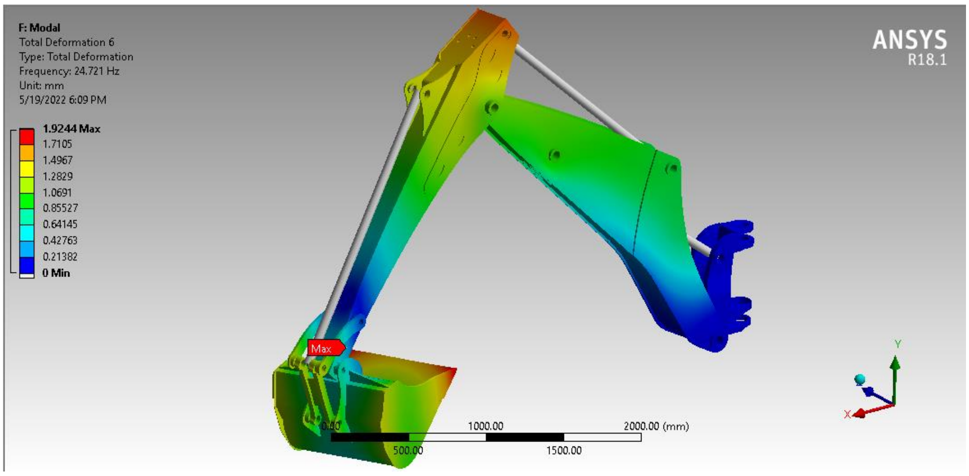

Figure 4.11. Modal Analysis Result On Mode 6

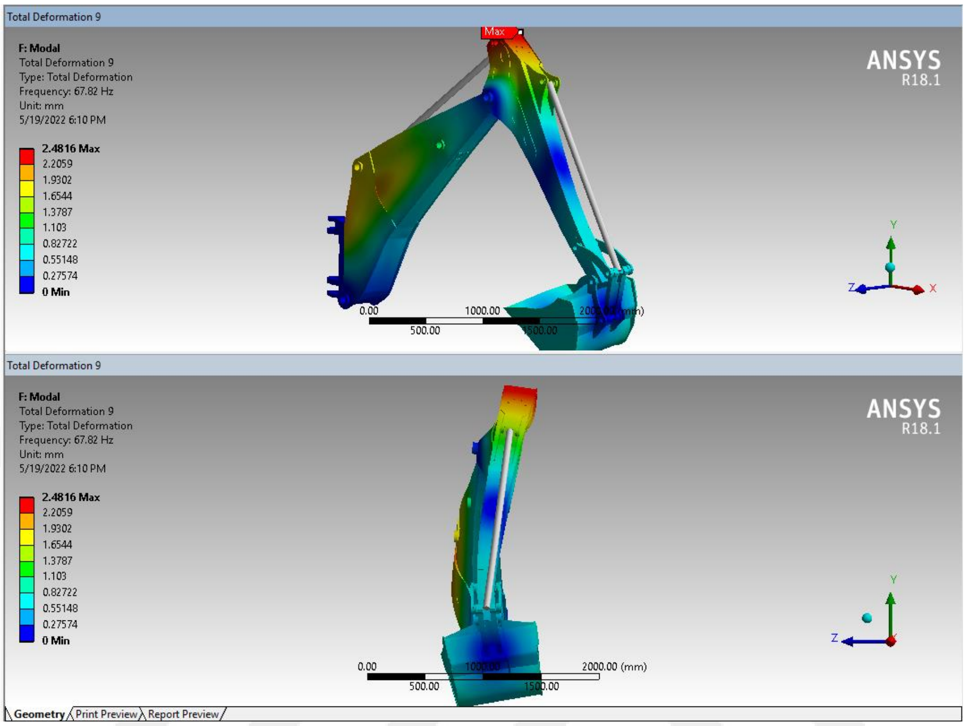

Figure 4.12. Modal Analysis Result On Mode 9

4.2.3. Random Vibration Analysis Results for New Backhoe Design

In the random vibration analysis, the equivalent stresses occurring after the PSD loads applied to the structure were examined and the fatigue damage values were calculated. It has been determined whether this damage value is higher than 1. In the regions where the highest stresses occur, it has been interpreted in accordance with the examinations whether fractures or cracks will occur.

4.2.3.1. Random Vibration Transverse Results for New Backhoe Design

In the lateral direction land scenario (See Fig. 3.22), when the random vibration analysis results of the lightened backhoe design are examined, the highest equivalent stress value on the structure was observed as 127.85 MPa, as seen in Figure 4.13. It has been determined that this stress value is well below the yield strength of the relevant material (S355J2). It has been determined that the region where the high stresses are concentrated is the region where the stick design group is connected with the boom design group with the revolute joint, and the details of the stresses in this region are given in Figure 4.14. When the high stress regions are examined, it is thought that the equivalent stresses are close to each other and the vibration loads in the Z axis direction cause the stresses to accumulate in this region in the backhoe design.

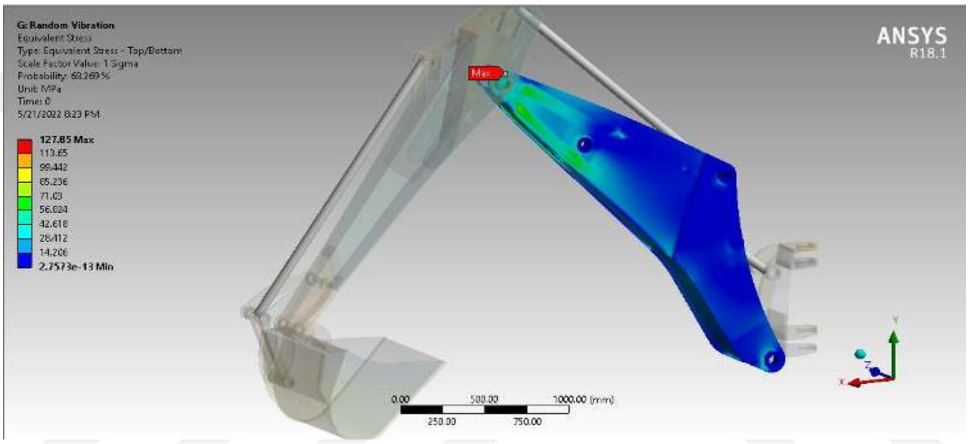

Figure 4.13. Random Vibration Transverse Analysis Results for New Backhoe Design

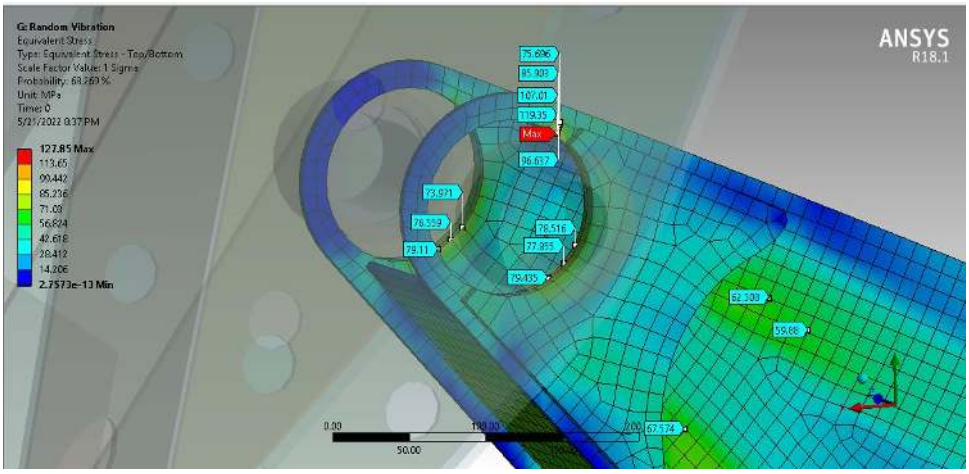

Figure 4.14. Random Vibration Transverse Analysis Results for High Stress Area

As a result of applying lateral vibration loads to the design for 3600s, the deformations in the boom design group have been determined and are shared in Figure 4.15 and Figure 4.16. The deformation severity was determined as a maximum of 0.30954, which was below 1. It was determined that the lightened backhoe design group remained in the area safely under lateral vibration loads.

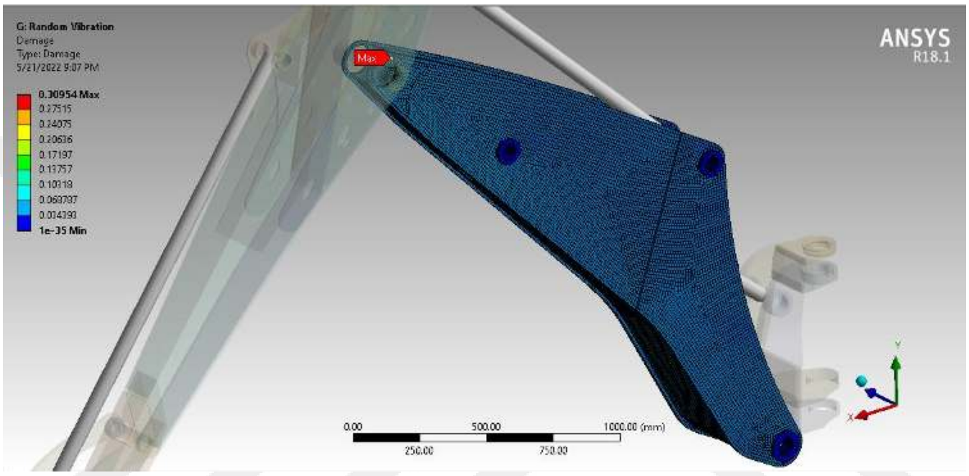

Figure 4.15. Random Vibration Transverse Analysis Results for Damage

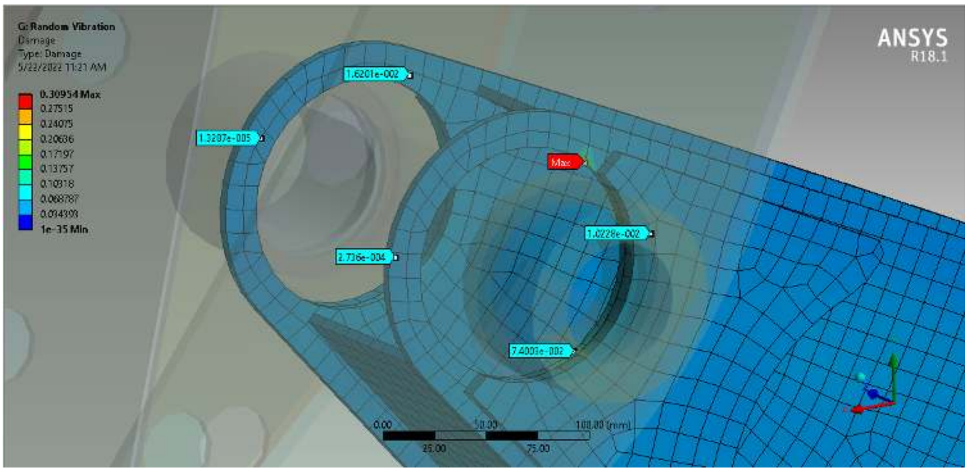

Figure 4.16. Random Vibration Transverse Analysis Results for Damage

4.2.3.2. Random Vibration Longitudinal Results for New Backhoe Design

When the random vibration analysis results of the lightened backhoe design in the linear direction land scenario were examined, the highest equivalent stress value on the structure was observed as 37.942 MPa. This stress value of the relevant material (See Table 3.1) is well below the yield strength. With the fixation, the lightened backhoe design remains in the safe zone under linear vibration loads. The regions where high stress occurs on the design are given in detail in Figures 4.17 and 4.18.

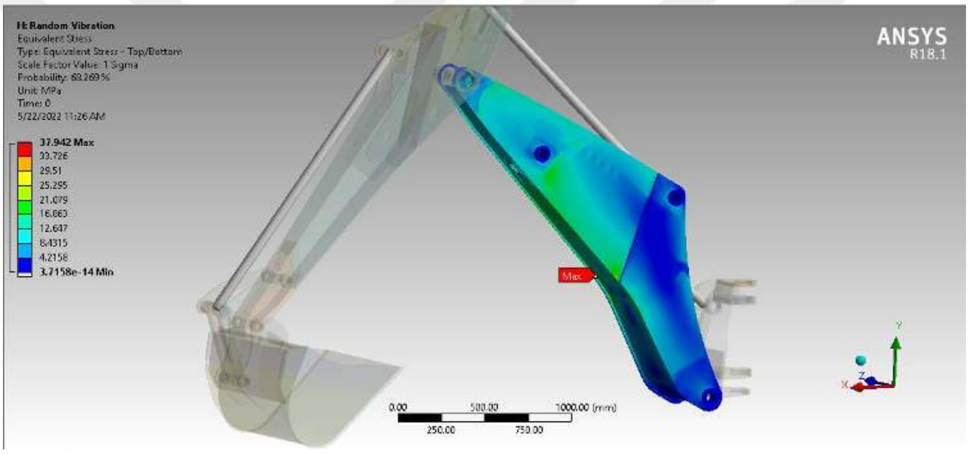

Figure 4.17. Random Vibration Long Analysis Results for New Backhoe Design

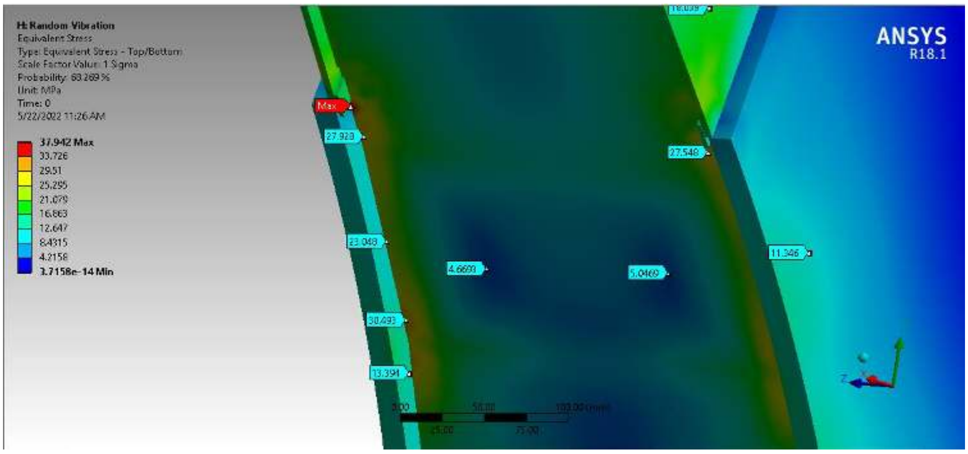

Figure 4.18. Random Vibration Longitudinal Analysis Results for High Stress Area

As a result of applying linear vibration loads to the design for 3600 s, the damages in the boom design group have been determined and the relevant images are shared in Figure 4.19 and Figure 4.20. Damage severity was determined as 0.0185 maximum, which was below 1. It was determined that the damage values that the lightened backhoe design group was exposed to linear vibration loads remained in the safe region.

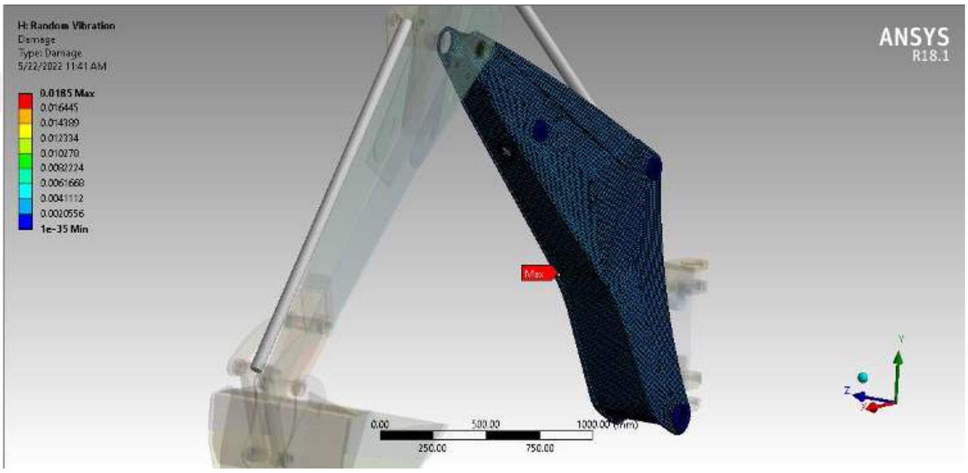

Figure 4 19. Random Vibration Longitudinal Analysis Results for Damage

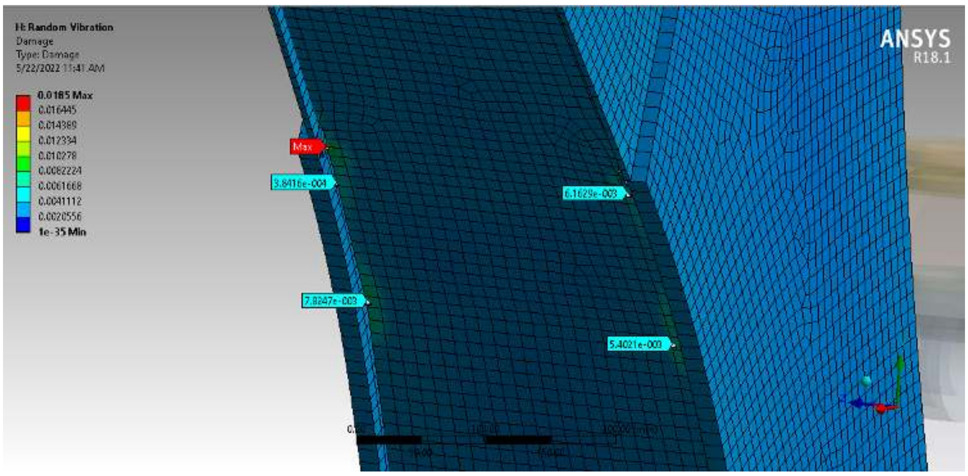

Figure 4.20. Random Vibration Longitudinal Analysis Results for Damage

4.2.3.3. Random Vibration Vertical Results for New Backhoe Design

When the random vibration analysis results of the lightened backhoe design in the vertical land scenario were examined, the highest equivalent stress value on the structure was observed as 218.82 MPa. It has been determined that the equivalent stresses occurring in the vertical vibration analysis is higher than the maximum equivalent stress value occurring in the lateral and linear direction vibration analysis. This is thought to be due to the backhoe design under full load, the critical position referenced in the model, and the boundary conditions. The determined maximum equivalent stress value of the relevant material (See Table 3.1) is below the yield strength. With the fixation, the lightened backhoe design remains in the safe zone under vertical vibration loads. The regions where high stress occurs on the design are given in detail in Figures 4.21 and 4.22.

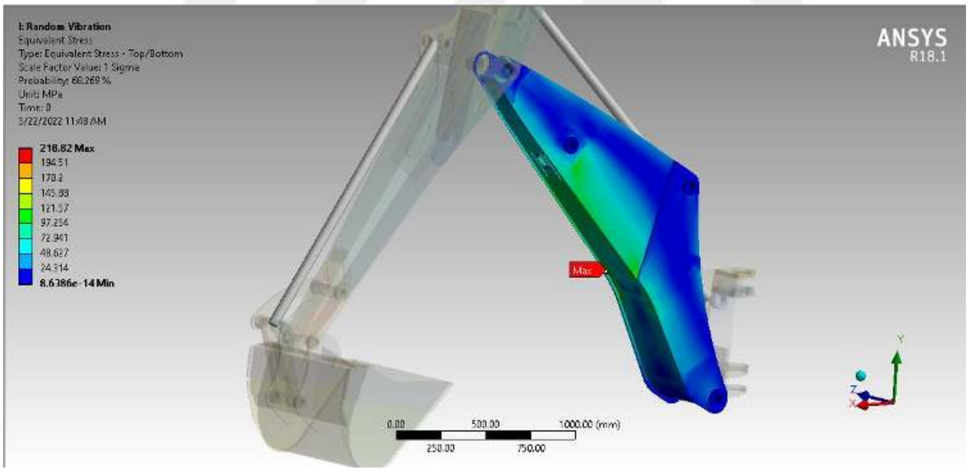

Figure 4.21. Random Vibration Vertical Analysis Results for New Backhoe Design

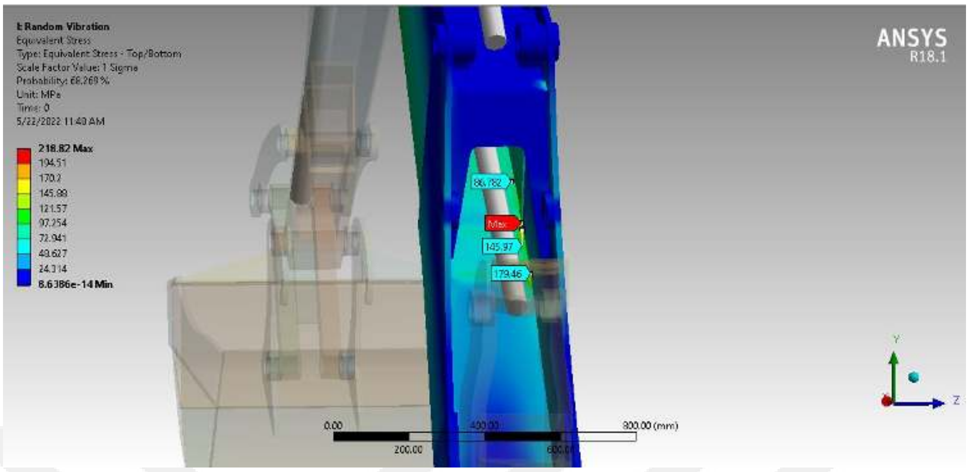

Figure 4.22. Random Vibration Vertical Analysis Results for High Stress Area

As a result of the application of vertical vibration loads to the design for 3600 s, the damages in the boom design group have been determined and the relevant images are shared in Figure 4.23 and Figure 4.24. The damage severity was determined as a maximum of 0.85321, which was below 1. It was determined that the damage values that the lightened backhoe design group was exposed to vertical vibration loads remained in the safe region.

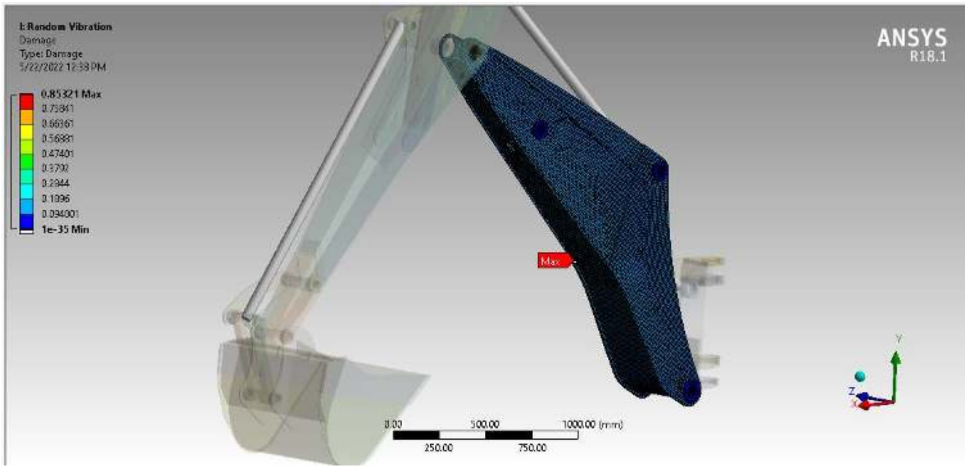

Figure 4.23. Random Vibration Vertical Analysis Results for Damage

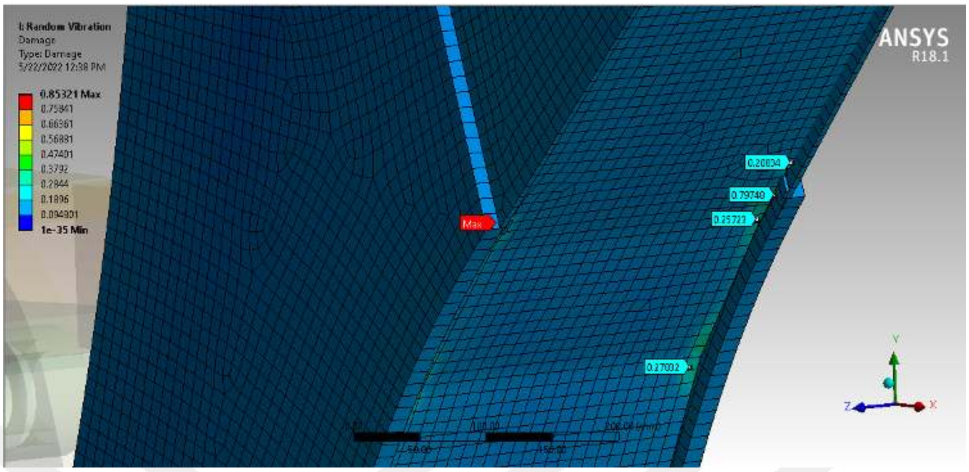

Figure 4.24. Random Vibration Vertical Analysis Results for Damage

4.2.4. Shock Analysis Results for Backhoe New Design

In this section, on the lightened backhoe design, under 15.2g 11 ms sawtooth shock loads in all 3 axes, X, Y and Z (See Fig. Figure 3.25), the equivalent stresses were examined over time. At the same time, the highest equivalent stress occurred during the analysis period was determined. Lateral, linear and vertical shock analysis results were analyzed separately for the lightweight backhoe design and compared with the yield strength of the relevant material. The analyses were evaluated together with the visuals in the shock analysis results.

4.2.4.1. Transient Analysis Transverse Shock Results for Backhoe New Design

As a result of the shock analysis of the lightened backhoe design carried out in the lateral direction, the maximum equivalent stress value observed on the structure was observed as 721.39 MPa. The observed maximum stress value was determined above the yield strength of the relevant material. However, since the high equivalent stresses detected are not distributed on the structure, it will not pose a problem in terms of structural integrity. In the lateral shock analysis results, it has been determined that the areas where high stresses occur in the boom design group occur at the junction of the boom wall sheet and the boom lower cross member sheet, and at the junction of the stick design group and the revolute joint of the boom design group. The highest equivalent stress occurred was read as 308.74 MPa at the junction of the boom wall sheet and the boom lower cross member sheet. In addition, the highest stress was read as 584.39 MPa in the region where the boom design group was connected with the stick and the revolute joint, and it was observed that it was close to the highest equivalent stress. Detailed images of the results are given in Figures 4.25, 4.26, 4.27 and 4.28.

Equivalent stresses occurring over time in the dampened boom design group during the lateral shock analysis period are given in Figure 4.26. When the graph is examined, it has been determined that the backhoe design is exposed to the highest stress at the time of 5.8e-2 under lateral shock loads and after this time it starts to dampen. The ability of the backhoe design to be able to absorb is an indication that it remains in the safe zone under lateral shock loads.

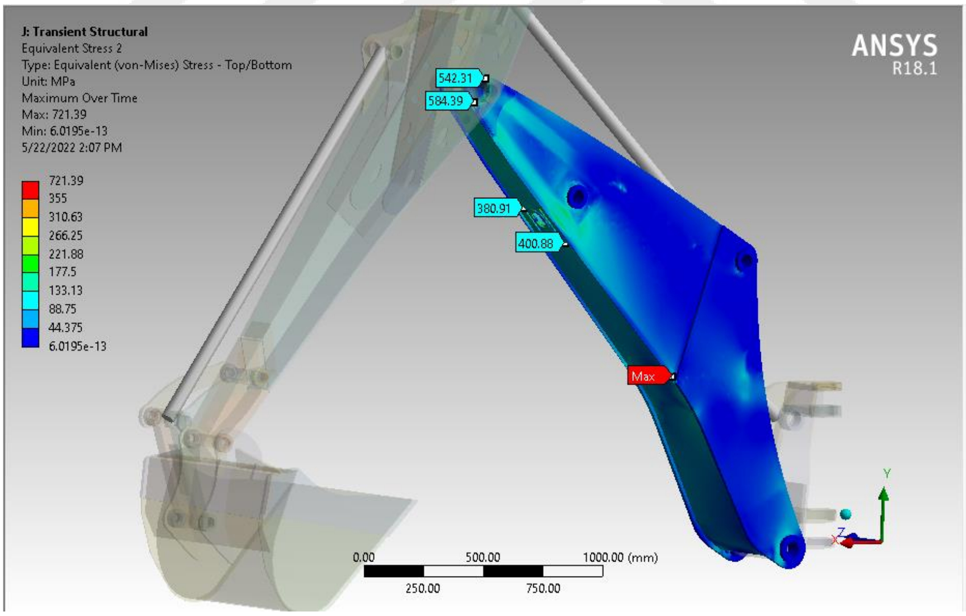

Figure 4.25. Transverse Shock Analysis Results for Backhoe New Design

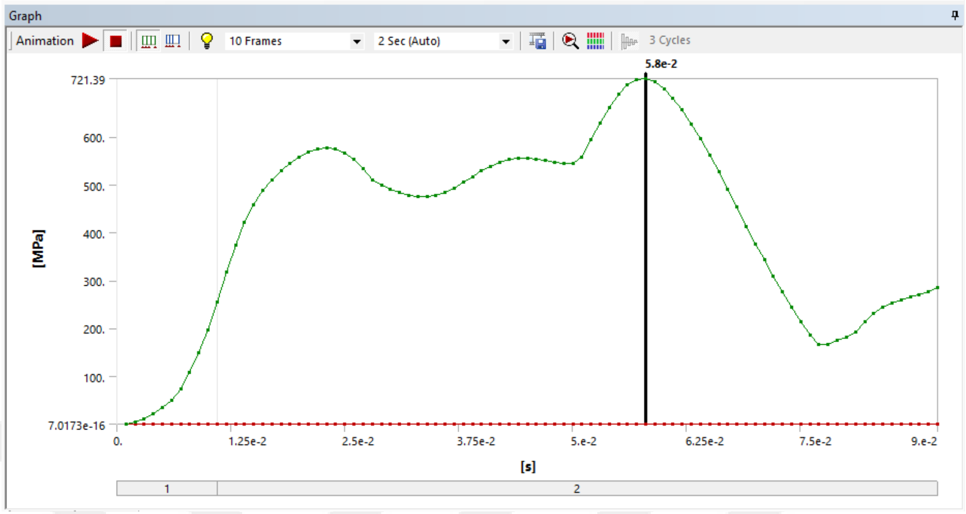

Figure 4.26. Transverse Shock Analysis σ-t Graph

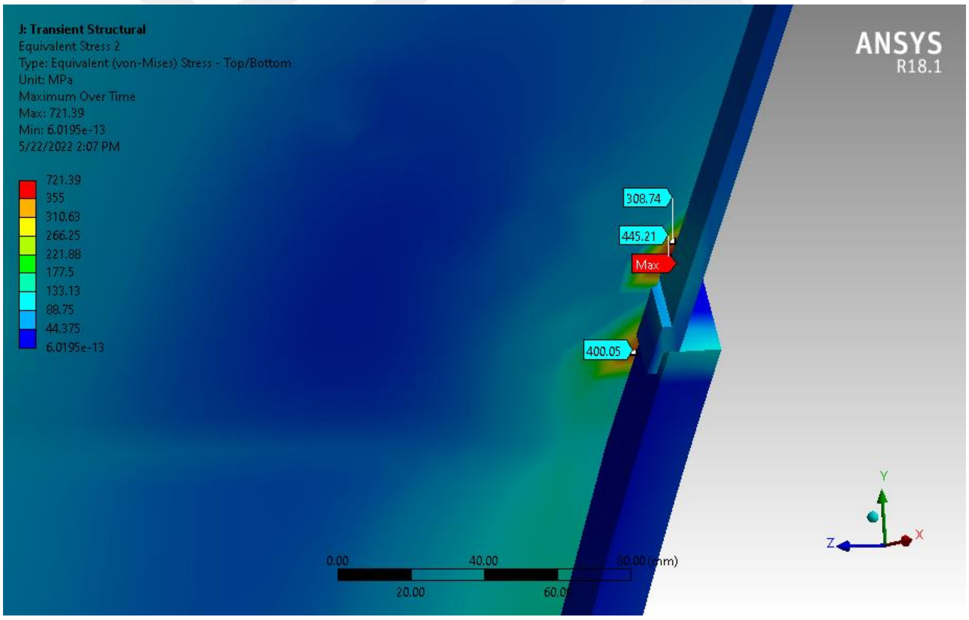

Figure 4.27. Transverse Shock Analysis Results High Stress Area 1

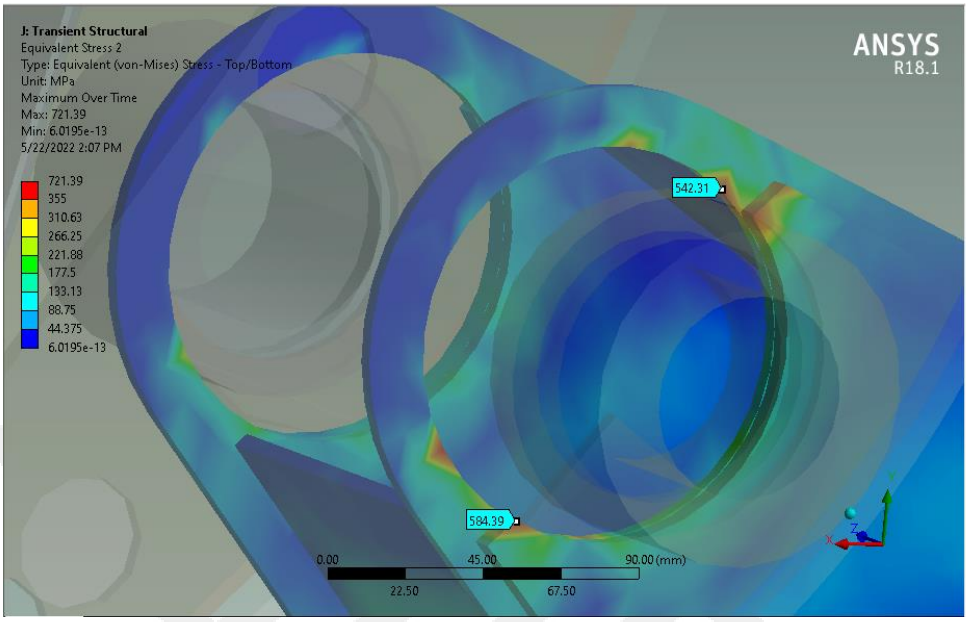

Figure 4.28. Transverse Shock Analysis Results High Stress Area 2

4.2.4.2. Transient Analysis Longitudinal Shock Results for Backhoe New Design

As a result of the shock analysis of the relieved backhoe design carried out in the linear direction, the maximum equivalent stress value observed on the structure was observed as 592.99 MPa. The observed maximum equivalent stress was determined above the yield strength of the material concerned. Although the determined maximum equivalent stress value is above the yield strength of the relevant material, it does not pose a problem in terms of structural integrity since it is not spread over the structure. In the linear direction shock analysis results, it was determined that the region where high stresses occurred in the boom design group occurred at the junction of the stick design group and the revolution joint of the boom design group.

This region, where high stresses occur, is examined in detail in Figures 4.29 and 4.30. The region where the high stresses occur is thought to be caused by the singularity in the finite element method, as can be seen in Figure 4.30. It has been observed that lower equivalent stresses such as 316.77 MPa occur at the other joints following the nodal points where the highest stress of 592.99 MPa occurs.

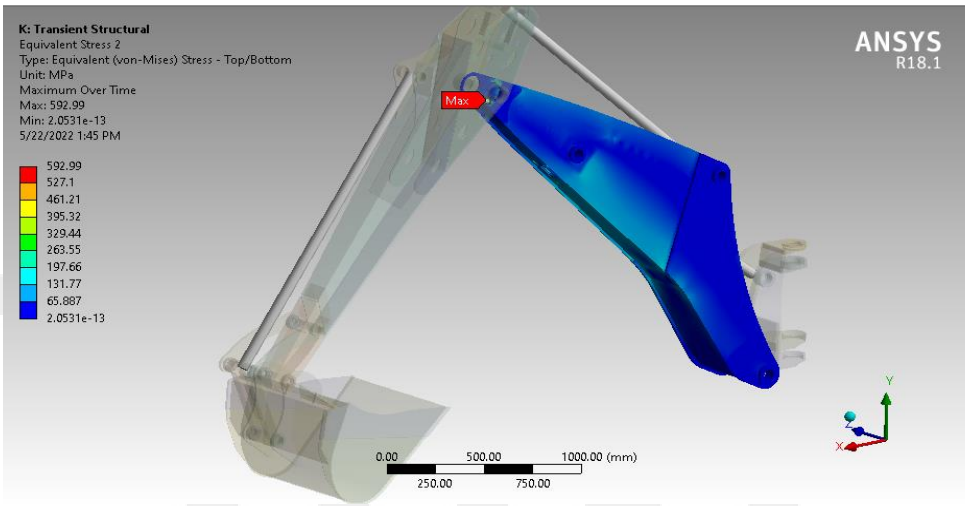

Figure 4.29. Longitudinal Shock Analysis Results for Backhoe New Design

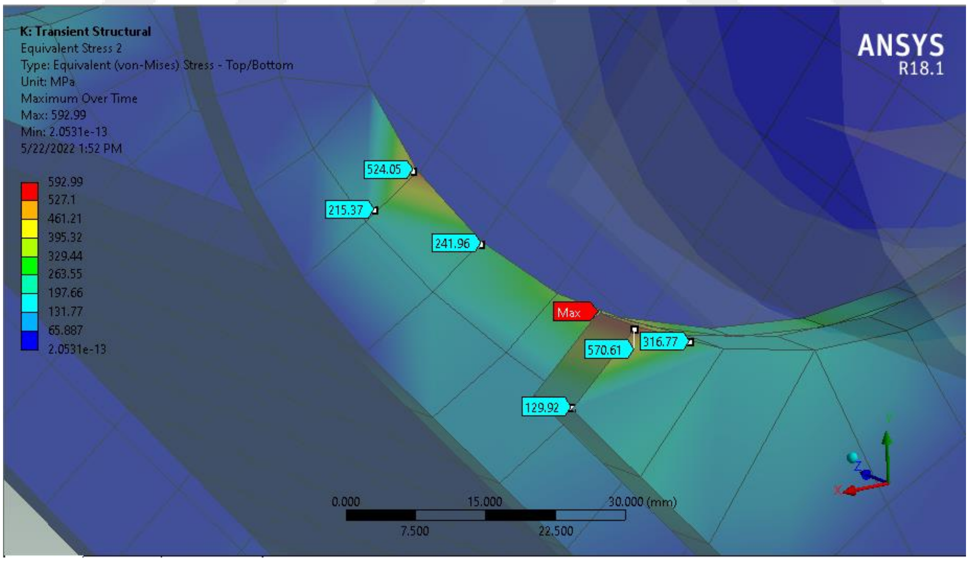

Figure 4.30. Longitudinal Shock Analysis Results for High Stress Area

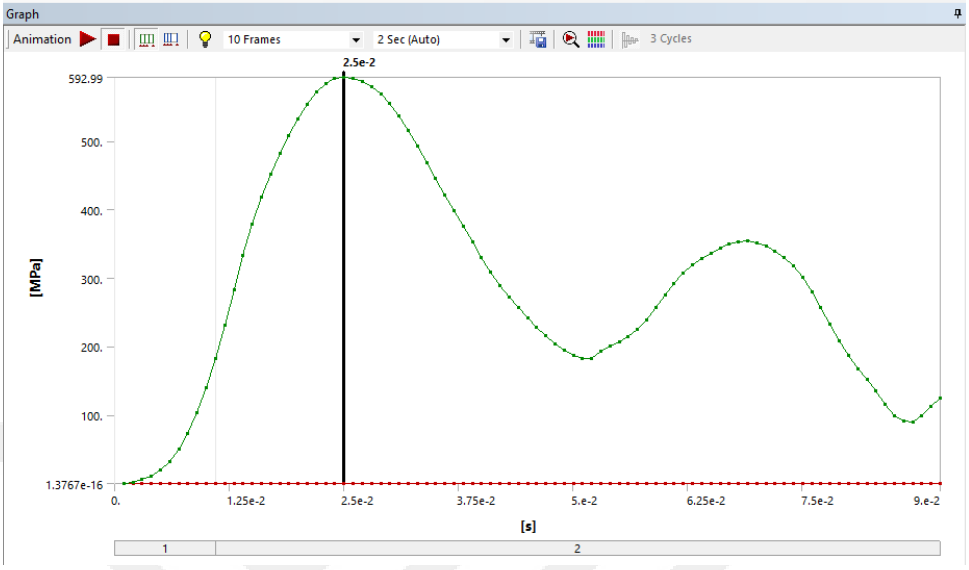

Figure 4.31. Longitudinal Shock Analysis σ-t Graph

Equivalent stresses occurring over time in the attenuated boom design group during the linear shock analysis period are given in Figure 4.31. When the graph is examined, it has been determined that the backhoe design is exposed to the highest stress at the time of 2.5e-2 under linear shock loads and after this time it starts to dampen. The ability of the backhoe design to be able to absorb is an indication that it remains in the safe zone under linear directional shock loads.

4.2.4.3. Transient Analysis Vertical Shock Results for Backhoe New Design

As a result of the shock analysis of the lightened backhoe design carried out in the vertical direction, the maximum equivalent stress value observed on the structure was observed as 677.19 MPa. The observed maximum equivalent stress was determined above the yield strength of the material concerned. Although the determined maximum equivalent stress value is above the yield strength of the relevant material, it does not pose a problem in terms of structural integrity since it is not spread over the structure. In the linear direction shock analysis results, it was determined that the areas where high stresses occur in the boom design group occur at the junction of the boom wall sheet and the boom lower cross member sheet, and at the junction of the boom design group with the stick design group and the revolute joint.

As can be seen in Figure 4.32 and Figure 4.33, the resulting stresses are mostly due to the singularity and are not distributed on the structure. The higher stresses following the maximum equivalent stress are studied in detail in Figure 4.33 and read as 650.81 MPa.

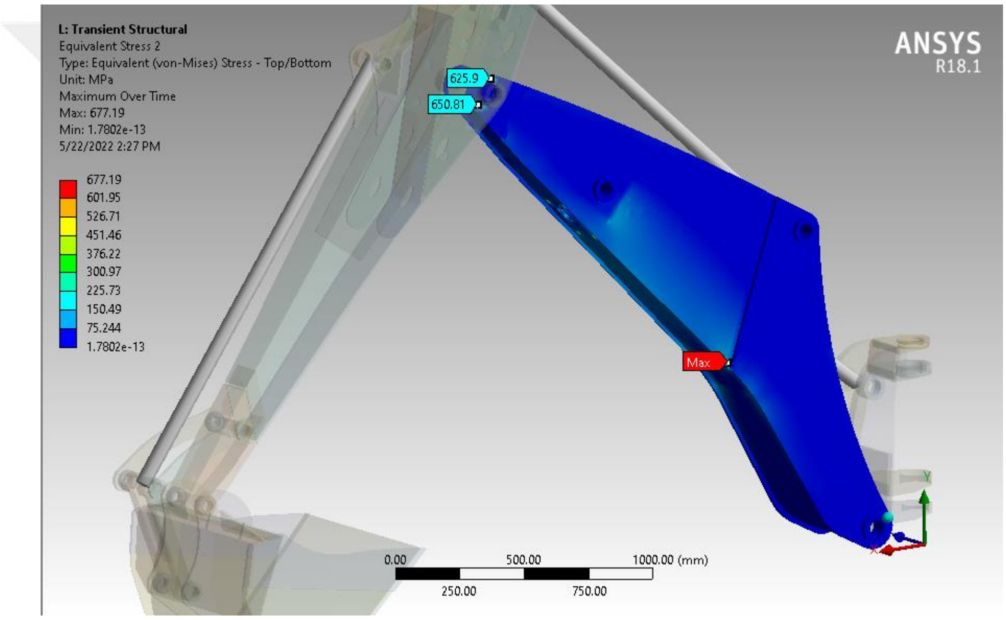

Figure 4.32. Vertical Shock Analysis Results for Backhoe New Design

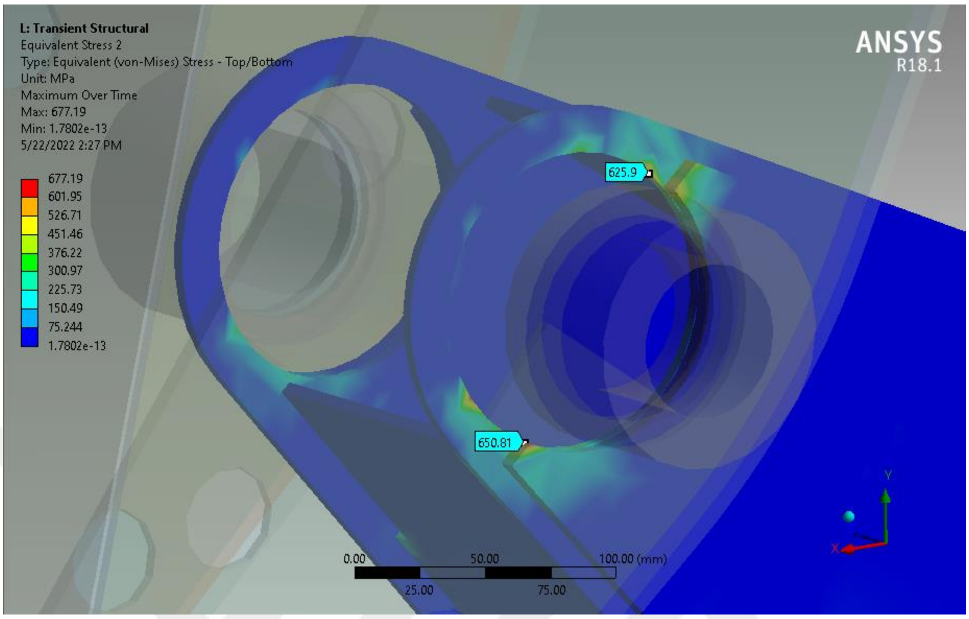

Figure 4.33. Vertical Shock Analysis Results High Stress Area

Equivalent stresses occurring over time in the attenuated boom design group during the vertical shock analysis period are given in Figure 4.34. When the graph is examined, it has been determined that the backhoe design is exposed to the highest stress at the time of 5.6e-2 under vertical shock loads and after this time it starts to dampen. Compared to lateral and linear shock equivalent stress-time graphs, we can say that the damping occurs later and the design is more difficult under vertical shock loads. In addition, the fact that the backhoe design can dampen is an indication that it remains in the safe zone under vertical shock loads.

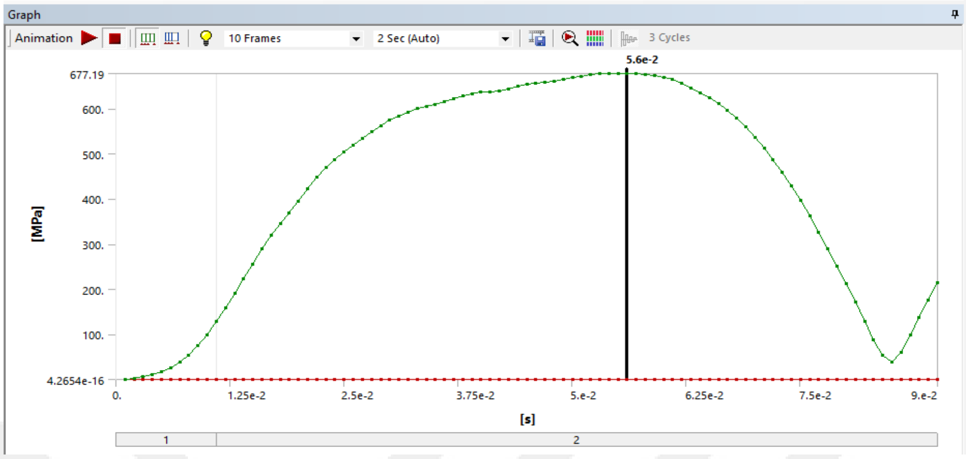

Figure 4.34. Vertical Shock Analysis σ-t Graph

We can see the static structural maximum equivalent stress and weight values of the current backhoe design and the new backhoe design in Table 4.3. There is an equivalent stress increase of 6.27% in the backhoe design after 32 kg of weight reduction.

Table 4.3. Results Value

	Weight of Modified Parts(kg)	Static Structural Result(MPa)
Current Backhoe Design	154	43.6
New Backhoe Design	122	46.3
	decrease 20.77%	increase 6.27%

5. CONCLUSIONS AND RECOMMENDATIONS

5.1. Conclusions

In this thesis, the backhoe design of a backhoe loader machine has been analyzed under full load operating conditions with the finite element method and design improvement studies have been carried out in line with the analysis. First of all, the existing backhoe design was analyzed in a dynamic environment and the critical position was determined with the help of time-dependent animations, then static analysis was carried out on the model established with reference to the critical position, and weight reduction studies were directed. The thickness of the boom wall sheet and boom lower cross member sheets in the backhoe design have been reduced by 4 mm, resulting in a total of 32 kg of lightening. (See. Table 3.7) The lightweight backhoe design was remodeled under the same boundary conditions with reference to the previously determined critical position, and static, modal, random vibration and shock analyses were performed, respectively, in accordance with military standards. With the help of the results of the analyses carried out on the new design, it was determined how the weight reduction effort affected the structural integrity of the backhoe design and safety controls were made.

5.1.1. Static Structural for Backhoe New Design

The solution was carried out under the specified boundary conditions, under the effect of gravity, under its own weight and 475 kg loading. Under this loading, a maximum stress of 46.601 MPa was observed for the existing backhoe design in the structure. The maximum total deformation value on the boom design group was determined as 1.9727 mm. The resulting maximum stress values of the materials of the construction (See. Table 3.1) does not pose any problem for the structure since it is below the yield strengths.

5.1.2. Modal Analysis Results for Backhoe New Design

The frequency modes formed in line with the boundary conditions applied for the modal analysis were given in Table 4.2 before. According to these results, modal analysis results were obtained with a total of 30 modes in the lightened backhoe design. Among the solution models, the lowest frequency was obtained as 6.0541 Hz, and effective mass participations were achieved above 90%, making it ready for modal, vibration and shock analysis.

5.1.3. Random Vibration Analysis for Backhoe New Design

Equivalent stresses determined in the results of all 3 analysis of the lightweight backhoe design, which were analyzed with vibration profiles in the lateral, linear and vertical directions, respectively, (See Table 3.1) was lower than the yield strength. It has been determined that the deformation results obtained by applying the vibration loads to the design for 3600 s for each axis are below 1. According to the random vibration analysis results, it has been determined that the backhoe design remains in the safe zone in terms of military standards.

5.1.4. Transient Structural Shock Analysis for Backhoe New Design

Equivalent time-dependent stresses were examined in the lightweight backhoe design, which was analyzed with shock loads in the lateral, linear and vertical directions, respectively, and stress-time graphs were examined. Finding the maximum equivalent stress values as 721.39 MPa, 592.99 MPa and 677.19 MPa, respectively, the equivalent stresses of the related material constituting the design (See Table 3.1) was found to be higher than the yield strength. When the detailed figures of the vibration analysis results were examined in Figures 4.25, 4.27, 4.28, 4.29, 4.30, 4.32 and 4.33, it was observed that the stresses that occur were not spread over the design and were due to the singularity frequently encountered in the finite element method. It was foreseen that the high equivalent stresses detected would not disrupt the structural integrity in the design, and the lightweight backhoe design was found to conform to military standards in terms of structure under operating conditions.

5.2. Recommendations

It is thought that it would be beneficial to support the results of the structural analysis performed after the weight reduction effort, in accordance with the military standards, before mass production, to support the field tests. If the prototype machine passes the tests successfully, it is predicted that a company that produces 600 to 1000 backhoe loaders annually will make much more profit with the lightweight design.

In addition to static, modal, random vibration and dynamic-based shock analyses performed with Ansys Workbench program modules, life cycle analyses can be performed in the future as a more detailed study. Detailed life cycle analyses can be made with one of the finite element programs that make calculations by adding the axial stresses preferred in the market to numeric approaches, and it can be determined how the lightening on the design responds in the long term under working conditions.

REFERENCES

Bhoomkar S., U., 2017. Finite Element Analysis and Optimization of Boom of Backhoe Loader. IJSRD - International Journal for Scientific Research and Development,5(10): 380-388.

Erklig, A. and Yeter, E., 2013. The Improvements of the Backhoe-Loader Arms. Modeling and Numerical Simulation of Material Science, 3(4): Article ID:37536,7 pages.

Fıçıcı, F., Yener, M., Arıkoğlu, T., Söylemez, E., 2003. Performing Experimental Strength Analysis Based on Finite Element Analysis Results in Construction Machinery Constructions. In Proceedings of 1st Construction Equipment Symposium and Exhibition, 236-245.

Frimpong, S., 2007. Stress Loading of the Cable Shovel Boom Under İn- Situ Digging Conditions” Engineering Failure Analysis, 14(4): 702-715.

İpek, L., 2006, Optimization Of Backhoe Loader Mechanism. MSc Thesis, Middle East Technical University, Ankara, 71p.

Kılınç, B., 2009, Dynamic Modelling Of A Backhoe Loader. MSc Thesis, Middle East Technical University, Ankara, 82p.

Kocabıyık, R., K., 2010, Bir İş Makinesi Kabinine Uygulanan Dinamik Analizlerin Bilgisayar Ortamında Simülasyonu. MSc Thesis, Yıldız Technical University, İstanbul, 85p.

Lee, H., Chang, Si and Lin, K., 2005. A Study of The Design, Manufacture and Remote Control of a Pneumatic Excavator. International Journal of Mechanical Engineering Education, 32(4): 345-361.

Lim, O., 2005. An Approximate Optimization Method for Large-Scaled Design Problem by Distributed Process Based on The Internet. World Congress of Structural and Multidisciplinary Optimization, Brasil.

Lüye, M., Sarıgeçili, İ., Pesen, E., 2022. Structural Investigation of Backhoe Design of Backhoe Loader with Finite Element Method Based Dynamic Analysis.

In Proceedings of VII. International Battalgazi Scientific Studies Congress, Malatya, Turkey, 532-543.

Oyman, V., 2005, Ekskavatör Kollarının Tasarımı, MSc Thesis, Yıldız Technical University, Istanbul, 71p.

Özer, S., 2007. Kazıcı-Yükleyicilerde Kazma Mesafesine Bağlı Olarak Bom-Stik Grubunun Tasarımı, MSc Thesis, Mersin University, Mersin, 77p.

Özsaraç, E., 2016. Stress Analysis and Improvement of Boom and Arm of an Excavator, MSc Thesis, University of Gaziantep, Gaziantep, 80p.

Özünlü, Ö. M., 2009. Dynamic Modeling Of An Excavator During Digging and Simulating The Motion, MSc Thesis, Middle East Technical University, Ankara, 136p.

Sharma, A., 2005. Kinematics and Finite Element Analysis of Excavator Attachments, PhD Thesis, Nirma University of Science and Technology, Ahmedabad.

Tewari, S., K., Dubey, J. and Chauhan, P., 2020. Modelling, FEA & Optimization of Backhoe Excavator attachment for max. Machine Life. SSRG International Journal of Mechanical Engineering, 7(2): 5-15.

Thorat, A., Rao S. and Munjal. S., 2013. Vibration Analysis of Loader Backhoe chassis 770 Model. International Journal of Engineering Sciences & Research Technology, 2(8): 2211-2216.

Vaniya, H., K., Sonara, V. D. and Sorthiya, A., S., 2015. Analysis of Backhoe Loader Chassis for Weight &Cost Reduction using FEA. IJIRST - International Journal for Innovative Research in Science & Technology, 1(8): 1-8.

Yener, M., 2003. Finite Element Analysis in Computer Environment and Its Importance in the Design of Construction Machinery Constructions. In Proceedigs of Construction Machinery Symposium and Exhibition, İstanbul, Turkey, 350-360.

Yeter, E., 2009. Improvement of backhoe-loader back and front arms, MSc Thesis, Gaziantep University, Gaziantep, p95.

Qureshi J., H. and Sagar, M., 2012. The Finite Element Analysis of Boom of Backhoe Loader. International Journal of Engineering Research and Applications, 2(3): 1484-1487.

Xiaohuo, L., Qingdi. C., Yongcheng. M. and Tianyu. Y., 2012. Finite element analysis of working mechanism for full hydraulic backhoe loader. In Proceedings of 2nd International Conference on Electronic & Mechanical Engineering and Information Technology, China: 2143-2146.

CURRICULUM VITAE

Mert Lüye graduated from high school in 2012 and started his university education at Eskişehir Osmangazi University in Eskişehir. He studied English in the preparatory class between 2012-2013 and started the Mechanical Engineering Department in 2013. He graduated from mechanical engineering in 2017. While working as an R&D engineer at Makinsan Trailer Company between 2018-2021, he started his graduate education in Çukurova University Mechanical Engineering Department in 2020. He worked as an R&D engineer at ÇÜMİTAŞ Company between 2021-2022. In March 2022, he has started to work as a structural analysis engineer at Koluman Otomotiv Endüstri A.Ş.

APPENDIX

A-1 Modal Analysis Results Participation Factor

Mode	Frequency(Hz)	X Direction	Y Direction	Z Direction	Rotation X	Rotation Y	Rotation Z
1	6.0541	-2.24E-03	1.14E-04	0.90296	826.07	-1383.6	1.5351
2	7.5945	-0.17078	0.88802	-9.11E-04	-3887.4	-745.59	1510.4
3	11.322	-0.63635	-0.25561	-3.81E-03	1113.1	-2778.8	-34.398
4	19.714	-0.71992	0.26195	2.39E-03	-1139.8	-3151.9	1348.4
5	21.198	-4.45E-04	-1.75E-03	0.37913	1057.1	-291.38	-4.6211
6	24.721	4.05E-03	-6.64E-04	0.45243	1108.4	184.71	-4.8054
7	48.781	6.72E-03	-1.14E-04	-0.17487	-256.48	-283.05	-9.7371
8	49.815	-2.84E-02	1.86E-04	-1.20E-02	-17.589	-145.9	41.014
9	67.82	4.98E-03	-1.81E-04	0.16476	69.621	286.35	-6.906
10	95.007	4.39E-04	-1.82E-03	-6.66E-05	7.9002	1.8406	0.34792
11	110.45	0.24882	3.31E-02	-1.03E-02	-154.23	1091.2	-318.9
12	115.33	-0.19233	-2.87E-02	-9.76E-03	114.49	-838.13	245.68
13	118.14	-2.27E-02	-1.60E-02	-4.33E-03	56.389	-87.074	43.089
14	125.67	-1.22E-02	7.99E-04	-1.62E-03	-16.151	-32.885	12.835
15	128.6	1.67E-02	-7.01E-03	-1.33E-03	91.627	-30.373	-11.646
16	135.43	-5.11E-02	1.31E-02	-1.75E-02	-9.2702	-310.9	41.962
17	141.02	0.22988	-7.74E-02	-2.31E-03	340.28	1000.3	-158.38
18	144.37	5.98E-02	-1.10E-02	-1.07E-02	53.307	237.02	-51.24
19	156.17	8.41E-02	0.11436	-2.62E-03	-503.87	366.08	-214.66
20	158.55	7.21E-03	1.29E-02	6.02E-02	-0.78534	67.745	-22.815
21	160.06	-2.56E-02	-2.52E-02	2.05E-03	112.09	-110.7	54.62
22	161.71	4.32E-03	2.75E-03	-1.12E-02	-11.189	-1.3153	-7.3734
23	165.75	2.33E-03	3.06E-04	2.63E-03	0.12058	11.056	-2.5398
24	182.76	2.57E-03	3.98E-03	-1.45E-04	-17.785	10.219	-6.9853
25	189.19	-1.95E-03	-1.15E-02	0.10258	110.08	97.16	16.084
26	198.15	5.57E-02	0.1011	1.12E-02	-435.43	254.75	-172.58
27	201.75	0.1564	0.30039	3.14E-02	-1293.7	716.66	-507.4
28	204.59	4.34E-02	8.81E-02	2.44E-02	-366.76	208.42	-146.22
29	209.09	-0.17831	-0.38142	8.26E-02	1731.1	-698.1	630.97
30	216.68	0.15011	0.35582	6.88E-02	-1501.9	728.12	-579.35

A-2 Modal Analysis Result Effective Mass

Mode	Frequency(Hz)	X Direction	Y Direction	Z Direction	Rotation X	Rotation Y	Rotation Z
1	6.0541	5.00E-06	1.31E-08	0.81533	6.82E+05	1.91E+06	2.3565
2	7.5945	2.92E-02	0.78858	8.30E-07	1.51E+07	5.56E+05	2.28E+06
3	11.322	0.40494	6.53E-02	1.45E-05	1.24E+06	7.72E+06	1183.2
4	19.714	0.51829	6.86E-02	5.71E-06	1.30E+06	9.93E+06	1.82E+06
5	21.198	1.98E-07	3.07E-06	0.14374	1.12E+06	84900	21.355
6	24.721	1.64E-05	4.41E-07	0.20469	1.23E+06	34120	23.092
7	48.781	4.52E-05	1.30E-08	3.06E-02	65782	80120	94.811
8	49.815	8.05E-04	3.45E-08	1.44E-04	309.38	21286	1682.1
9	67.82	2.48E-05	3.29E-08	2.71E-02	4847.1	81999	47.693
10	95.007	1.93E-07	3.32E-06	4.44E-09	62.413	3.3879	0.12105
11	110.45	6.19E-02	1.10E-03	1.06E-04	23786	1.19E+06	1.02E+05
12	115.33	3.70E-02	8.22E-04	9.53E-05	13107	7.02E+05	60358
13	118.14	5.16E-04	2.57E-04	1.87E-05	3179.7	7581.9	1856.7
14	125.67	1.50E-04	6.39E-07	2.61E-06	260.86	1081.4	164.74
15	128.6	2.80E-04	4.91E-05	1.77E-06	8395.4	922.52	135.63
16	135.43	2.61E-03	1.71E-04	3.06E-04	85.936	96657	1760.8
17	141.02	5.28E-02	5.99E-03	5.36E-06	1.16E+05	1.00E+06	25083
18	144.37	3.57E-03	1.21E-04	1.14E-04	2841.6	56178	2625.5
19	156.17	7.07E-03	1.31E-02	6.86E-06	2.54E+05	1.34E+05	46079
20	158.55	5.20E-05	1.67E-04	3.62E-03	0.61676	4589.4	520.54
21	160.06	6.54E-04	6.36E-04	4.18E-06	12564	12255	2983.3
22	161.71	1.86E-05	7.59E-06	1.26E-04	125.18	1.7301	54.367
23	165.75	5.41E-06	9.37E-08	6.90E-06	1.45E-02	122.23	6.4507
24	182.76	6.63E-06	1.58E-05	2.10E-08	316.29	104.43	48.794
25	189.19	3.79E-06	1.33E-04	1.05E-02	12117	9440.1	258.68
26	198.15	3.10E-03	1.02E-02	1.26E-04	1.90E+05	64896	29785
27	201.75	2.45E-02	9.02E-02	9.88E-04	1.67E+06	5.14E+05	2.57E+05
28	204.59	1.88E-03	7.75E-03	5.94E-04	1.35E+05	43439	21382
29	209.09	3.18E-02	0.14548	6.82E-03	3.00E+06	4.87E+05	3.98E+05
30	216.68	2.25E-02	0.12661	4.73E-03	2.26E+06	5.30E+05	3.36E+05

A-3 Modal Analysis Results Cumulative Effective Mass

Mode	Frequency(Hz)	X Direction	Y Direction	Z Direction	Rotation X	Rotation Y	Rotation Z
1	6.0541	4.15E-06	9.89E-09	0.65235	2.40E-02	7.57E-02	4.37E-07
2	7.5945	2.42E-02	0.59498	6.52E-01	5.55E-01	9.77E-02	4.23E-01
3	11.322	0.36064	6.44E-01	6.52E-01	5.99E-01	4.03E-01	0.42359
4	19.714	0.7912	6.96E-01	6.52E-01	6.44E-01	7.96E-01	7.61E-01
5	21.198	7.91E-01	6.96E-01	0.76737	6.84E-01	0.79934	0.761
6	24.721	7.91E-01	6.96E-01	0.93114	7.27E-01	0.80069	0.76101
7	48.781	7.91E-01	6.96E-01	9.56E-01	0.72925	0.80386	0.76103
8	49.815	7.92E-01	6.96E-01	9.56E-01	0.72926	0.8047	0.76134
9	67.82	7.92E-01	6.96E-01	9.77E-01	0.72943	0.80794	0.76135
10	95.007	7.92E-01	6.96E-01	9.77E-01	0.72943	0.80794	0.76135
11	110.45	8.43E-01	6.97E-01	9.78E-01	0.73027	8.55E-01	7.80E-01
12	115.33	8.74E-01	6.98E-01	9.78E-01	0.73073	8.83E-01	0.79142
13	118.14	8.75E-01	6.98E-01	9.78E-01	0.73084	0.88312	0.79176
14	125.67	8.75E-01	6.98E-01	9.78E-01	0.73085	0.88316	0.7918
15	128.6	8.75E-01	6.98E-01	9.78E-01	0.73115	0.8832	0.79182
16	135.43	8.77E-01	6.98E-01	9.78E-01	0.73115	0.88702	0.79215
17	141.02	9.21E-01	7.02E-01	9.78E-01	7.35E-01	9.27E-01	0.7968
18	144.37	9.24E-01	7.02E-01	9.78E-01	0.73532	0.92881	0.79729
19	156.17	9.30E-01	7.12E-01	9.78E-01	7.44E-01	9.34E-01	0.80584
20	158.55	9.30E-01	7.12E-01	9.81E-01	0.74424	0.9343	0.80594
21	160.06	9.30E-01	7.13E-01	9.81E-01	0.74469	0.93478	0.80649
22	161.71	9.30E-01	7.13E-01	9.81E-01	0.74469	0.93478	0.8065
23	165.75	9.30E-01	7.13E-01	9.81E-01	7.45E-01	0.93478	0.8065
24	182.76	9.30E-01	7.13E-01	9.81E-01	0.7447	0.93479	0.80651
25	189.19	9.30E-01	7.13E-01	9.89E-01	0.74513	0.93516	0.80656
26	198.15	9.33E-01	7.21E-01	9.89E-01	7.52E-01	0.93773	0.81209
27	201.75	9.53E-01	7.89E-01	9.90E-01	8.11E-01	9.58E-01	8.60E-01
28	204.59	9.55E-01	7.95E-01	9.91E-01	8.15E-01	0.95976	0.86383
29	209.09	9.81E-01	0.90447	9.96E-01	9.21E-01	9.79E-01	9.38E-01
30	216.68	1.00E+00	1	1.00E+00	1.00E+00	1.00E+00	1.00E+00

A-4 Transverse Shock Analysis Result By Time

Time(s)	Min. Equivalent Stress(Mpa)	Max. Equivalent Stress(Mpa)
1.00E-03	7.02E-16	0.80576
2.00E-03	3.65E-15	4.1651
3.00E-03	5.84E-15	11.03
4.00E-03	1.11E-14	21.027
5.00E-03	1.57E-14	33.92
6.00E-03	2.17E-14	50.665
7.00E-03	3.68E-14	73.746
8.00E-03	5.69E-14	107.05
9.00E-03	7.64E-14	148.14
1.00E-02	9.61E-14	197.46
1.10E-02	1.22E-13	255.1
1.20E-02	1.65E-13	316.57
1.30E-02	2.28E-13	373.37
1.40E-02	2.82E-13	420.73
1.50E-02	2.97E-13	458.23
1.60E-02	2.81E-13	487.23
1.70E-02	2.72E-13	510.07
1.80E-02	2.85E-13	528.86
1.90E-02	3.05E-13	544.66
2.00E-02	3.07E-13	557.68
2.10E-02	2.87E-13	567.62
2.20E-02	2.68E-13	573.96
2.30E-02	2.66E-13	576.12
2.40E-02	2.76E-13	573.51
2.50E-02	2.85E-13	565.69
2.60E-02	2.93E-13	552.48
2.70E-02	3.09E-13	533.96
2.80E-02	3.37E-13	510.47
2.90E-02	3.25E-13	498.83
3.00E-02	3.22E-13	490.84
3.10E-02	2.71E-13	483.42

3.20E-02	2.13E-13	477.9
3.30E-02	9.52E-14	474.78
3.40E-02	8.86E-14	474.32
3.50E-02	1.57E-13	477.03
3.60E-02	1.38E-13	483.37
3.70E-02	1.24E-13	493.06
3.80E-02	1.15E-13	504.83
3.90E-02	1.10E-13	517.04
4.00E-02	1.13E-13	528.43
4.10E-02	1.16E-13	538.34
4.20E-02	1.15E-13	546.37
4.30E-02	1.09E-13	552
4.40E-02	9.99E-14	554.82
4.50E-02	9.08E-14	554.88
4.60E-02	8.97E-14	552.89
4.70E-02	1.09E-13	549.88
4.80E-02	1.49E-13	546.83
4.90E-02	2.04E-13	544.44
5.00E-02	2.64E-13	544.27
5.10E-02	3.26E-13	557.68
5.20E-02	3.88E-13	593.95
5.30E-02	3.94E-13	629.37
5.40E-02	3.85E-13	661.64
5.50E-02	3.84E-13	688.6
5.60E-02	3.84E-13	708.33
5.70E-02	3.78E-13	719.43
5.80E-02	3.69E-13	721.39
5.90E-02	3.66E-13	714.71
6.00E-02	3.69E-13	700.64
6.10E-02	3.73E-13	680.58
6.20E-02	3.72E-13	655.7
6.30E-02	3.61E-13	626.96
6.40E-02	3.47E-13	595.33
6.50E-02	3.34E-13	561.76
6.60E-02	3.23E-13	526.94

6.70E-02	3.06E-13	490.92
6.80E-02	2.43E-13	453.04
6.90E-02	1.90E-13	412.41
7.00E-02	1.72E-13	375.36
7.10E-02	1.42E-13	342.74
7.20E-02	4.20E-14	309.13
7.30E-02	8.39E-14	275.5
7.40E-02	8.39E-14	243.01
7.50E-02	2.61E-14	212.99
7.60E-02	5.78E-14	186.77
7.70E-02	3.79E-14	165.57
7.80E-02	5.26E-14	166.89
7.90E-02	7.66E-14	175.69
8.00E-02	1.01E-13	180.94
8.10E-02	1.26E-13	192.77
8.20E-02	1.28E-13	214.84
8.30E-02	1.32E-13	231.53
8.40E-02	1.37E-13	243.89
8.50E-02	1.44E-13	253.07
8.60E-02	1.49E-13	260.02
8.70E-02	1.47E-13	265.5
8.80E-02	1.46E-13	270.07
8.90E-02	1.50E-13	276.1
9.00E-02	1.45E-13	284.66

A-5 Long Shock Analysis Result By Time

Time(s)	Min. Equivalent Stress(Mpa)	Max. Equivalent Stress(Mpa)
1.00E-03	1.38E-16	0.40168
2.00E-03	5.49E-16	2.052
3.00E-03	1.91E-15	5.5692
4.00E-03	1.55E-15	11.242
5.00E-03	3.87E-15	19.503
6.00E-03	4.67E-15	31.442
7.00E-03	3.16E-15	49.748
8.00E-03	7.58E-15	73.743
9.00E-03	1.91E-14	103.73
1.00E-02	3.25E-14	140.07
1.10E-02	3.84E-14	183.19
1.20E-02	5.21E-14	231.86
1.30E-02	4.83E-14	282.7
1.40E-02	7.92E-14	332.41
1.50E-02	8.04E-14	378.26
1.60E-02	1.06E-13	418.27
1.70E-02	1.07E-13	452.2
1.80E-02	1.04E-13	481.36
1.90E-02	9.28E-14	507.56
2.00E-02	9.96E-14	531.82
2.10E-02	1.13E-13	553.7
2.20E-02	1.35E-13	571.72
2.30E-02	1.37E-13	584.39
2.40E-02	1.54E-13	591.23
2.50E-02	1.63E-13	592.99
2.60E-02	1.60E-13	591.04
2.70E-02	1.49E-13	586.39
2.80E-02	1.44E-13	579.17
2.90E-02	1.52E-13	568.74
3.00E-02	1.66E-13	554.45
3.10E-02	1.72E-13	536.29

3.20E-02	1.65E-13	515.06
3.30E-02	1.54E-13	492.09
3.40E-02	1.53E-13	468.59
3.50E-02	1.53E-13	445.09
3.60E-02	1.45E-13	421.29
3.70E-02	9.73E-14	399.08
3.80E-02	7.05E-14	376.19
3.90E-02	6.45E-14	352.58
4.00E-02	6.74E-14	329.55
4.10E-02	8.55E-14	308.22
4.20E-02	9.11E-14	289.04
4.30E-02	9.11E-14	271.87
4.40E-02	9.14E-14	256.26
4.50E-02	8.71E-14	241.72
4.60E-02	8.28E-14	228.02
4.70E-02	7.71E-14	215.25
4.80E-02	7.47E-14	203.78
4.90E-02	6.07E-14	194.21
5.00E-02	6.84E-14	187.09
5.10E-02	5.27E-14	182.69
5.20E-02	6.00E-14	183.1
5.30E-02	6.60E-14	192.62
5.40E-02	5.37E-14	200.64
5.50E-02	3.72E-14	207.11
5.60E-02	3.13E-14	214.24
5.70E-02	3.67E-14	224.55
5.80E-02	3.13E-14	239.05
5.90E-02	4.47E-14	256.66
6.00E-02	6.51E-14	275.08
6.10E-02	5.64E-14	292.12
6.20E-02	3.96E-14	306.65
6.30E-02	3.29E-14	318.56
6.40E-02	4.32E-14	328.35
6.50E-02	7.74E-14	336.63
6.60E-02	6.63E-14	343.71

6.70E-02	6.79E-14	349.39
6.80E-02	7.00E-14	353.04
6.90E-02	7.07E-14	353.95
7.00E-02	6.10E-14	351.81
7.10E-02	5.06E-14	346.92
7.20E-02	4.96E-14	339.73
7.30E-02	5.62E-14	330.2
7.40E-02	4.77E-14	317.58
7.50E-02	3.29E-14	300.94
7.60E-02	5.10E-14	280.17
7.70E-02	5.13E-14	256.5
7.80E-02	4.55E-14	232.04
7.90E-02	3.29E-14	208.57
8.00E-02	2.75E-14	186.48
8.10E-02	2.78E-14	167.87
8.20E-02	2.17E-14	152.14
8.30E-02	1.74E-14	134.59
8.40E-02	1.16E-14	115.21
8.50E-02	1.14E-14	99.51
8.60E-02	2.12E-14	91.098
8.70E-02	2.06E-14	90.285
8.80E-02	2.23E-14	98.678
8.90E-02	2.70E-14	112.51
9.00E-02	3.55E-14	124.2

A-6 Vertical Shock Analysis Results By Time

Time(s)	Min. Equivalent Stress(Mpa)	Max. Equivalent Stress(Mpa)
1.00E-03	4.27E-16	0.60116
2.00E-03	2.13E-15	2.7048
3.00E-03	4.84E-15	6.1405
4.00E-03	5.66E-15	10.578
5.00E-03	3.36E-15	16.332
6.00E-03	1.23E-14	24.913
7.00E-03	1.25E-14	37.682
8.00E-03	1.31E-14	54.339
9.00E-03	1.18E-14	74.831
1.00E-02	1.64E-14	99.24
1.10E-02	2.31E-14	128.08
1.20E-02	2.89E-14	159.59
1.30E-02	3.37E-14	190.84
1.40E-02	2.11E-14	222.37
1.50E-02	3.15E-14	255.44
1.60E-02	5.88E-14	288.62
1.70E-02	7.02E-14	318.97
1.80E-02	6.53E-14	345.32
1.90E-02	4.29E-14	369.67
2.00E-02	5.15E-14	394.8
2.10E-02	8.21E-14	421.35
2.20E-02	9.08E-14	447.12
2.30E-02	8.25E-14	469.27
2.40E-02	5.87E-14	487.17
2.50E-02	5.92E-14	502.66
2.60E-02	8.41E-14	517.94
2.70E-02	1.00E-13	533.63
2.80E-02	9.03E-14	548.68
2.90E-02	7.29E-14	561.93
3.00E-02	7.36E-14	573.3
3.10E-02	9.50E-14	583.32

3.20E-02	1.09E-13	592.14
3.30E-02	1.02E-13	599.35
3.40E-02	8.77E-14	604.82
3.50E-02	8.54E-14	609.53
3.60E-02	1.01E-13	614.9
3.70E-02	1.19E-13	621.45
3.80E-02	1.22E-13	628.12
3.90E-02	1.20E-13	633.16
4.00E-02	1.20E-13	635.85
4.10E-02	1.28E-13	637.29
4.20E-02	1.36E-13	639.42
4.30E-02	1.34E-13	643.37
4.40E-02	1.34E-13	648.56
4.50E-02	1.40E-13	653.36
4.60E-02	1.51E-13	656.67
4.70E-02	1.59E-13	658.76
4.80E-02	1.59E-13	660.87
4.90E-02	1.49E-13	663.94
5.00E-02	1.49E-13	667.89
5.10E-02	1.57E-13	671.78
5.20E-02	1.68E-13	674.7
5.30E-02	1.70E-13	676.34
5.40E-02	1.58E-13	677.03
5.50E-02	1.49E-13	677.19
5.60E-02	1.52E-13	677.01
5.70E-02	1.69E-13	676.43
5.80E-02	1.66E-13	675.26
5.90E-02	1.65E-13	673.16
6.00E-02	1.48E-13	669.55
6.10E-02	1.45E-13	663.71
6.20E-02	1.55E-13	655.32
6.30E-02	1.57E-13	644.82
6.40E-02	1.52E-13	634.43
6.50E-02	1.40E-13	623
6.60E-02	1.34E-13	610.25

6.70E-02	1.47E-13	595.79
6.80E-02	1.42E-13	578.82
6.90E-02	1.33E-13	558.85
7.00E-02	1.28E-13	536.17
7.10E-02	1.08E-13	511.55
7.20E-02	1.15E-13	485.53
7.30E-02	1.12E-13	457.9
7.40E-02	1.02E-13	428.13
7.50E-02	9.56E-14	395.97
7.60E-02	9.09E-14	361.78
7.70E-02	7.98E-14	326.13
7.80E-02	7.68E-14	289.25
7.90E-02	6.37E-14	251.02
8.00E-02	5.13E-14	211.35
8.10E-02	4.82E-14	170.58
8.20E-02	4.37E-14	129.24
8.30E-02	2.70E-14	87.931
8.40E-02	1.65E-14	53.109
8.50E-02	4.54E-15	38.913
8.60E-02	1.18E-14	61.052
8.70E-02	2.03E-14	99.245
8.80E-02	3.11E-14	138.16
8.90E-02	1.88E-14	176.68
9.00E-02	1.90E-14	214.72